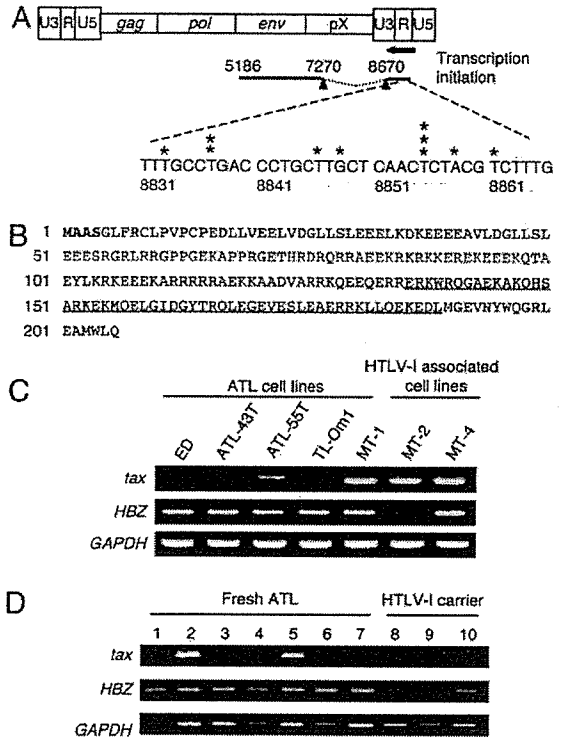

Fig. 1. *HBZ* gene expression in ATL cells. (*A*) 5′ RACE was performed by using total RNA from the ATL cell line ATL-55T. The schema represents the HTLV-I provirus and spliced *HBZ* mRNA. Asterisks show transcription initiation sites identified by 5′ RACE. The 3′ end of the transcript (5186) was identified by 3′ RACE, and polyadenylation signal was found upstream (5206–5211) of this transcript. Nucleic acids are numbered with reference to ATK-1 according to Seiki *et al.* (22). (*B*) Hypothetical amino acid sequence derived from spliced *HBZ*. Amino acids different from the previously reported HBZ are shown in bold type. The basic leucine zipper domain is underlined. (*C*) Expression of *tax* and *HBZ* genes in ATL and HTLV-I-immortalized cell lines analyzed by RT-PCR. (*D*) Expression of *tax* and *HBZ* genes in fresh ATL cells and peripheral blood mononuclear cells from HTLV-I carriers. Lanes: 1–7, fresh ATL cases; 8–10, peripheral blood mononuclear cells from HTLV-I carriers.

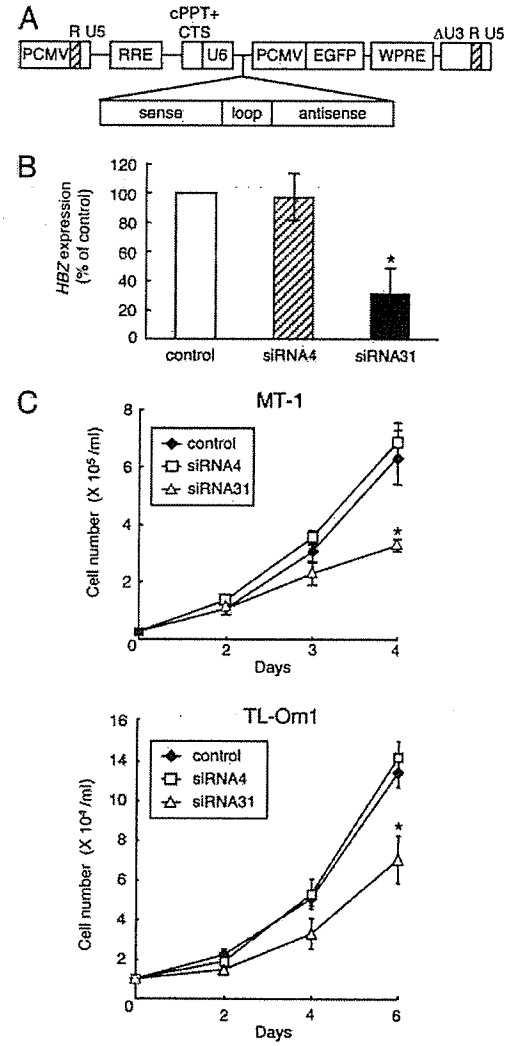

Fig. 2. Knockdown of *HBZ* gene expression inhibits cell growth of ATL cells. (*A*) Schematic diagram of the short hairpin RNA-expressing lentiviral vector. PCMV, immediate early cytomegalovirus promoter; RRE, Rev-responsive element; cPPT, central polypurine tract; CTS, central termination sequence; WPRE, woodchuck hepatitis virus posttranscriptional regulatory element. (*B*) siRNA31 decreases *HBZ* gene transcription, whereas siRNA4 does not (*Supporting Methods*, which is published as supporting information on the PNAS web site). Efficiencies of lentivirus vector transfection, which were determined by EGFP expression, were 99.3% and 93.0% for MT-1 and TL-Om1, respectively. *HBZ* transcripts in siRNA transfectants of MT-1 are quantified by a densitometer and shown as percentages compared with a mock transfectant. Values are means ± SD from three independent experiments. (*C*) Transfection of lentivirus vector expressing siRNA31 suppresses the growth of MT-1 and TL-Om1. The transfectants of siRNAs were harvested at day 7 after transfection, and seeded into a 96-well plate at 5×10^3 cells per well. Cell numbers of each transfectants were counted in triplicate by Trypan blue dye exclusion method. Values are means ± SD. *, $P < 0.05$.

disruptive genetic changes in any cell line or in fresh ATL samples (17 cases), except for polymorphisms (Table 1, which is published as supporting information on the PNAS web site).

Inhibition of *HBZ* by siRNA Suppresses Growth of ATL Cells. Although inhibition of Tax-mediated viral gene transcription has been reported as a function of HBZ (20), *HBZ* was expressed in ATL cells lacking *tax* gene transcription, suggesting that *HBZ* has other roles. To clarify the role of *HBZ* in ATL cells, we suppressed *HBZ* gene expression by using siRNAs. Recombinant lentiviruses transcribing short hairpin RNAs against *HBZ* under control of the U6 promoter (Fig. 2*A*) were generated and transduced to *tax*-expressing MT-1 and *tax*-nonexpressing TL-Om1 cells. In MT-1 cells, siRNA31 suppressed *HBZ* gene mRNA expression, whereas siRNA4 did not (Fig. 2*B*). Growth of both cell lines was suppressed by siRNA31 (Fig. 2*C*) along with *HBZ* transcription (Fig. 6, which is published as supporting information on the PNAS web site). Apoptosis was not induced by siRNA31. These findings indicate that *HBZ* gene expression is required for ATL cell proliferation, regardless of *tax* gene expression.

To analyze *HBZ* function, a vector expressing *HBZ* was transfected into Kit 225 cells, an IL-2-dependent human T cell line derived from T cell chronic lymphocytic leukemia cells (23), and stable transformants were selected in the presence of G418. *HBZ*-transfected Kit 225 cells showed prolonged survival after removal of IL-2 (Fig. 3*A*) compared with control cells, and *HBZ*-transduced Kit 225 cells showed an increase in the number of cells in S phase after depletion of IL-2 (Fig. 3*B*). In addition, *HBZ*-transfected Kit 225 cells showed enhanced responsiveness to IL-2 (Fig. 3*C*, WT). To identify *HBZ* target genes in Kit 225 cells, transcriptional profiles of *HBZ*-transfected and control cells after withdrawal of IL-2 (48 h) were analyzed by an

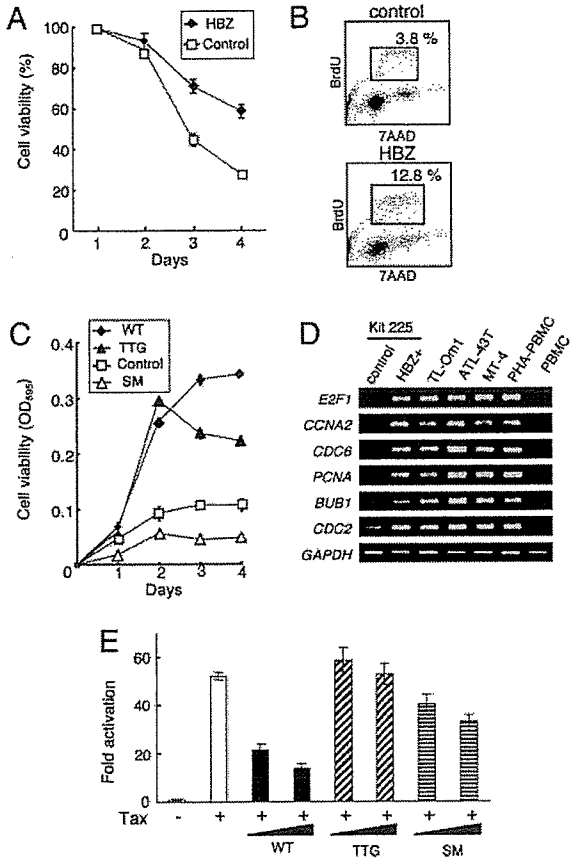

Fig. 3. Functional analyses of the *HBZ* gene. (*A*) *HBZ* gene expression prolongs survival of transfected Kit 225 cells after withdrawal of IL-2. Cell viabilities are measured with 3-(4,5-dimethylthiazol-2-yl)-2,5-diphenyl tetrazolium bromide assay. Values are means ± SD. (*B*) Cell cycle analyses of *HBZ*-expressing Kit 225 cells, and Kit 225 cells transfected with a control vector. Cells in S phase were identified by BrdUrd incorporation and staining with 7AAD after withdrawal of IL-2. (*C*) Effects of wild-type (WT) and mutant forms of *HBZ* on proliferation of IL-2-stimulated Kit 225 cells. A suboptimal level of IL-2 (2.5 units/ml) was added after removal of IL-2 (48 h), and cell viability was measured by an 3-(4,5-dimethylthiazol-2-yl)-2,5-diphenyl tetrazolium bromide assay. The first ATG of *HBZ* is mutated to TTG, which blocks synthesis of HBZ protein. All codons in the *HBZ* gene are replaced with silent mutations (SM). The sequence of SM *HBZ* has been shown in Fig. 7. (*D*) Semiquantitative RT-PCR analysis for differentially expressed genes in *HBZ*-expressing Kit 225 cells compared with control cells. (*E*) Effects of *HBZ* and its mutants on Tax-mediated transactivation through the HTLV-I LTR. Lusiferase reporter (WT-Luc) and Tax expressing vector were transfected into Jurkat cells with or without vectors expressing wild-type (WT) or mutated *HBZ* (TTG or SM) (0.3 or 1 μg). Fold activation were calculated compared with basal luciferase activity of WT-Luc. Results are means ± SD in triplicate.

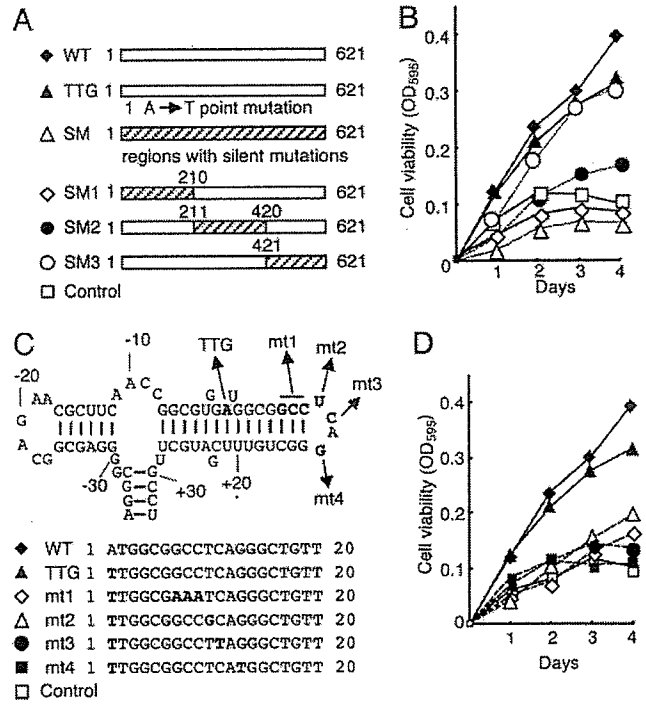

Fig. 4. Functional analyses of mutated *HBZ* genes on proliferation of T cells. (*A*) Schemas of mutant *HBZ* genes. (*B*) The effects of mutated *HBZ* genes on cell growth were measured by assays. The hatched area represents the region containing silent mutations. Numbers indicate the nucleotide positions in the *HBZ* coding sequence. (*C*) Predicted stem-loop structure in *HBZ* mRNA of the native *HBZ* gene (from −35 to +33). Nucleotides are numbered from the first ATG (A: +1) of the *HBZ* gene. Structural predictions were analyzed by using MFOLD (24). Mutated sequences of each vector are shown in bold type. (*D*) The results of 3-(4,5-dimethylthiazol-2-yl)-2,5-diphenyl tetrazolium bromide assays with these vectors are shown.

oligonucleotide microarray. We identified 687 genes up-regulated (by >2-fold) and 719 genes down-regulated (by >2-fold) in *HBZ*-transfected cells (Tables 2 and 3, which are published as supporting information on the PNAS web site). Expression of selected candidate genes was confirmed by RT-PCR (Fig. 3*D*), which indicated that transcription of the *E2F1* gene and its targets, *CCNA2*, *CDC6*, *PCNA*, *CDC2*, and *BUB1*, were up-regulated in *HBZ*-transfected Kit 225 cells. We speculated that up-regulation of *E2F1* is involved in enhanced proliferation mediated by *HBZ*.

To confirm whether HBZ protein promotes cell proliferation, we generated vectors expressing two *HBZ* gene mutants. Mutation that the first ATG of *HBZ* is replaced by TTG blocks synthesis of HBZ protein (TTG *HBZ*). Surprisingly, expression of TTG *HBZ* still promoted proliferation (Fig. 3*C*), suggesting that *HBZ* functions to promote cell proliferation as an RNA. To confirm this hypothesis, we replaced all coding regions in the *HBZ* gene with silent mutations (SM *HBZ*) (Fig. 7, which is published as supporting information on the PNAS web site). Such mutations completely altered the secondary structure of the RNA, but the SM *HBZ* gene still produced intact HBZ protein. SM *HBZ* gene expression did not promote cell proliferation (Fig. 3*C*), indicating that the growth-promoting effect of *HBZ* depended on RNA structure.

Because an inhibitory effect of HBZ on Tax-mediated transactivation through the 5′ LTR has been reported (20), we analyzed this function by using mutant forms of *HBZ*. As shown in Fig. 3*E*, wild-type *HBZ* suppressed Tax-mediated transactivation of transcription from the HTLV-I 5′ LTR. Although the SM *HBZ* gene also suppressed transactivation, TTG *HBZ* completely lacked this activity. Taken together, these findings suggest that *HBZ* promotes T cell proliferation in the form of RNA, whereas HBZ protein inhibits Tax-mediated transactivation through the 5′ LTR.

To further analyze the growth-promoting activity of *HBZ* RNA, we constructed vectors expressing a series of mutated *HBZ* genes (Fig. 4 *A* and *C*). When *HBZ* genes with silent mutations in different regions were analyzed, we found that mutations in the first 210 bp of *HBZ* (SM1) abolished growth-promoting activity (Fig. 4*B*). In addition, silent mutations in SM2 partially decreased growth-promoting activity of *HBZ*. When we compared the predicted secondary RNA structures of the native *HBZ* gene and the form of *HBZ* expressed in the pME18Sneo

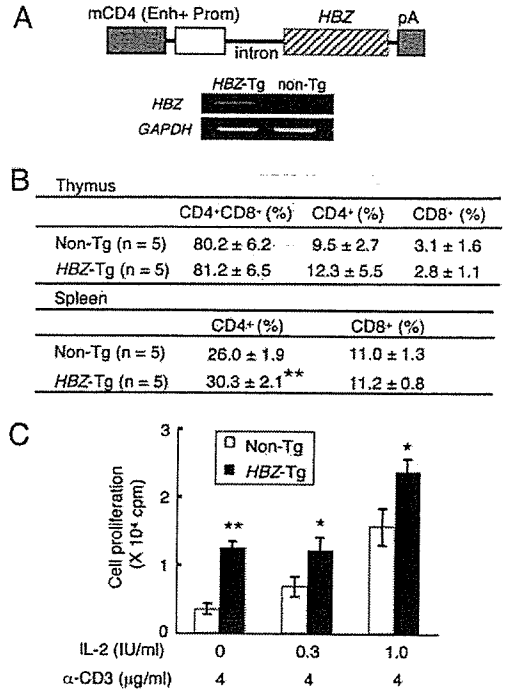

Fig. 5. Generation and analyses of *HBZ*-transgenic (Tg) mice. (*A*) Schematic representation of the *HBZ* transgene. The promoter (Prom) and enhancer (Enh) of the mouse CD4 (mCD4) gene were ligated to *HBZ* cDNA (including the 5′ UTR) plus the polyadenylation signal sequence of SV40. Expression of *HBZ* transcripts was detected by RT-PCR in purified $CD4^+$ splenocytes from *HBZ*-Tg mice. (*B*) T cell subsets in *HBZ*-Tg mice. Values are means ± SD from five transgenic mice. **, $P < 0.01$. (*C*) Proliferative responses of thymocytes from *HBZ*-Tg mice to IL-2 and/or stimulation with an anti-CD3 antibody. Proliferative responses were measured by ^{3}H-thymidine incorporation. ^{3}H-thymidine uptake of thymocytes without anti-CD3 antibody and IL-2 was 5.8 ± 4.6 cpm for control mice and 21.0 ± 16.0 cpm for *HBZ* transgenic mice. Values are means ± SD in triplicate. *, $P < 0.05$; **, $P < 0.01$.

vector, the first stem-loop of *HBZ* RNA was present in both cases (Fig. 4*C*). Although the TTG *HBZ* gene retained strong growth-promoting activity, TTG *HBZ* genes with mutations in the first stem-loop structure showed reduced or no activity (Fig. 4 *C* and *D*, mutants 1–4), indicating that it is essential for growth-promoting activity.

Microarray analyses of Kit 225 cells expressing wild-type and TTG *HBZ* genes identified transcriptional changes mediated by *HBZ* RNA, showing that RNA was responsible for up-regulation of *E2F1* (Table 2). Taken together, we conclude that the first stem-loop structure is important for growth-promoting activity of *HBZ*. To study the possibility that microRNA is responsible for growth-promoting activity, we performed Northern blot analysis by using oligonucleotides from the region containing the first stem-loop structure as probes. However, microRNA was not detected by Northern blot analysis (data not shown).

***In Vivo* Effect of *HBZ* Gene Expression in Transgenic Mice.** To analyze the role of *HBZ in vivo*, we generated transgenic mice expressing *HBZ* under the control of the mouse CD4 promoter/enhancer, which induces specific transgene expression in CD4-positive cells (Fig. 5*A*) (25). *HBZ* expression in transgenic mice was confirmed in CD4-positive splenocytes by RT-PCR (Fig. 5*A*). Thymocyte subpopulations in transgenic mice did not differ from those observed in nontransgenic littermates. However, the percentage of CD4-positive T lymphocytes increased in splenocytes of transgenic mice ($P < 0.01$) (Fig. 5*B*). In addition, proliferation induced by cross-linking with an immobilized anti-CD3 antibody was augmented in thymocytes of transgenic mice (Fig. 5*C*). These data indicate that the *HBZ* gene promotes proliferation of CD4-positive T lymphocytes *in vivo*.

Discussion

HTLV-I infection causes a fatal neoplastic disease, ATL, after a long latent period. Because transfection of retroviral vectors expressing *tax* can immortalize T lymphocytes *in vitro* (26), it has been suggested that *tax* plays a central role in oncogenesis among HTLV-I accessory genes. Tax has pleiotropic actions by interacting with cellular proteins, which promotes clonal proliferation of infected cells (2, 3). However, the role of the *tax* gene remains an enigma in ATL cells, because *tax* gene transcripts cannot be detected in ≈60% of ATL cases (12). However, the 3′ LTR and *HBZ* sequences are conserved in all ATL cells regardless of deletion or hypermethylation of the 5′ LTR or of genetic changes in the *tax* gene, suggesting that an intact 3′ LTR and *HBZ* gene are critical for oncogenesis. In this study, we showed that the *HBZ* gene encoded by the minus strand of the HTLV-I provirus is transcribed in all ATL cells. HBZ has been reported to suppress Tax-mediated transactivation of viral gene transcription through the 5′ LTR. In addition to this function, we showed that *HBZ* promotes proliferation of T lymphocytes *in vitro* and *in vivo*. These findings indicate that *HBZ* plays a critical role in oncogenesis mediated by HTLV-I, even in late stages of oncogenesis when *tax* is not expressed.

In oncogenic DNA viruses, oncoproteins, such as the SV40 T antigen and human papillomavirus E7 protein, target retinoblastoma (Rb) protein and inactivate its function (27). Loss of Rb function is associated with deregulation of E2F transcription factors (28). E2F1, a critical regulator of cell cycle progression, plays a pivotal role in the G_1-to-S-phase transition by transactivating specific target genes (29). Furthermore, overexpression of E2F1 has been reported to be associated with oncogenesis (30). As shown in this study, *HBZ* RNA increased *E2F1* gene transcription, which is likely associated with *HBZ*-induced proliferation. Although Tax was also reported to induce *E2F1* expression (31), *E2F1* is overexpressed in ATL cell lines lacking Tax expression, indicating that *HBZ* may be responsible for up-regulating *E2F1* expression.

Tax promotes cell growth and inhibits apoptosis of infected cells. However, because Tax is the major target of cytotoxic T lymphocytes, its expression is also disadvantageous to the survival of infected cells (17, 32). Therefore, HTLV-I encodes several other viral genes, such as *rex*, *p30*, and *HBZ*, to suppress Tax production by different mechanisms (20, 21, 33, 34). Because such suppression has a negative effect on growth of infected cells, the *HBZ* gene is likely to support proliferation of infected cells in addition to its activity in suppressing *tax* gene transcription. Because growth-promoting activity of *HBZ* could be a critical factor in maintaining a leukemic state, *HBZ* should be a therapeutic target.

Recently, microRNAs have been demonstrated to play important roles in regulating gene expression (35). Virus-encoded microRNAs have been also identified (36, 37), and some function in viral replication. In HIV-1, microRNAs have been demonstrated to function in viral transcription (38, 39). In HTLV-I, when *env* RNA is transcribed with the *HBZ* gene, such a long double-stranded RNA could be precursor for Dicer processing, resulting in formation of viral siRNAs. Such siRNA might function to suppress viral gene expression in HTLV-I. It is noteworthy that *HBZ* transcription is suppressed in MT-2 cells (Fig. 1*C*). In MT-2 cells, *env-tax* fusion gene is abundantly transcribed (15), which might generate siRNA and suppress *HBZ* expression.

Epstein–Barr virus (EBV)-encoded nonpolyadenylated RNA (also known as EBV-encoded small RNA or EBER) is known to

function in oncogenesis by activating transcription of genes such as insulin-like growth factor 1 (40) or interleukin 9 (41). Although these functional RNAs do not encode polypeptides, *HBZ* can function as both RNA and protein. Because of their limited genome size (8,506 bp for HTLV-I), complex retroviruses have evolved to use RNA splicing to express required genes. In addition to such a mechanism, HTLV-I not only expresses the *HBZ* gene on the minus strand but it also utilizes this gene as protein and RNA. Bimodal functions of viral gene may represent a previously uncharacterized strategy to regulate viral replication and proliferation of infected cells.

In conclusion, we showed that spliced *HBZ* gene was transcribed in all ATL cells. The *HBZ* gene promotes proliferation of ATL cells in the RNA form, whereas HBZ protein suppresses Tax-mediated viral transcription through the 5′ LTR. Although the role of *tax* gene remains undetermined in ATL cells, this study sheds light on the role of *HBZ* gene in oncogenesis.

Materials and Methods

Cells. Two HTLV-I immortalized lines (MT-2, and MT-4) and five ATL cell lines (ED, ATL-43T, ATL-55T, TL-Oml, and MT-1) were used in this study (15). The IL-2-dependent human T cell line Kit 225 was maintained in RPMI medium 1640 supplemented with 10% FBS and recombinant IL-2 (85 units/ml). Approval for this study was obtained from the institutional review board of Kyoto University. Informed consent was obtained from blood donors and patients according to the Declaration of Helsinki. To construct vectors encoding wild-type (WT) and mutant forms of *HBZ*, the coding sequence (621 bp) was amplified from cDNA of TL-Oml cells and subcloned into the pME18Sneo vector (42). Vectors were transfected into Kit 225 cells by using Nucleofector (Amaxa Biosystems, Cologne, Germany). Briefly, cells were suspended in 100 μl of Cell Line Nucleofector Solution T and then nucleofected with vectors (5 μg) by using program T-16 of the Nucleofector device (Amaxa Biosystems). Stable transfectants were selected in G418 (600 μg/ml).

Rapid Amplification of cDNA 5′and 3′ Ends (RACE). To determine the 5′ and 3′ ends of transcripts, RACE was performed by using the SMART RACE cDNA amplification kit (BD Biosciences Clontech) according to manufacturer's instructions (42). First-strand cDNAs were synthesized from 1 μg of total RNA of ATL-55T, ATL-43T, or MT-1 cells by reverse transcriptase and used for 5′ RACE PCR. For nested amplifications, primers specific for the *HBZ* gene (5′-CCTCTTTCTC-CCGCTCTTTTTTTCGC-3′ and 5′-CATGACACAG-GCAAGCATCGAAACA-3′) were used. For nested 3′ RACE amplifications, primers specific for the *HBZ* gene (5′-CTAGGTTAGGGCAGGGGGGCTGTAGGGC-3′ and 5′-GGGTCCACGAACAAACTGGCTGGGCAGG-3′) were used. PCR products were cloned into vectors, and the nucleotide sequences were determined.

Synthesis of cDNA and Semiquantitative RT-PCR. Spliced *HBZ*, *tax*, and *GAPDH* transcripts were quantified by using RT-PCR. The primers used were as follows: *HBZ* gene: 5′-TAAACTTACCTA-GACGGCGG-3′ (sense), 5′-CTGCCGATCACGATGCGTTT-3′ (antisense); *tax* gene: 5′-CCGGCGCTGCTCTCATCCCGGT-3′ (sense) and 5′-GGCCGAACATAGTCCCCCAGAG-3′ (antisense). PCR was performed in a PC-808 (Astec) under the following conditions: *HBZ*, 2 min at 95°C, followed by 35 cycles of 30 seconds at 95°C, 30 seconds at 57.5°C, and 30 seconds at 72°C; *tax*, 2 min at 95°C, followed by 35 cycles of 30 seconds at 95°C, 30 seconds at 61°C, and 30 seconds at 72°C. The intensity of PCR-amplified band was quantified by using ATTO densitograph 4.0 (Atto Instruments, Tokyo). Semiquantitative RT-PCR was performed to confirm microarray results by using primers (Table 4, which is published as supporting information on the PNAS web site).

Lentiviral Vector Construction and Transfection of Recombinant Lentivirus. We modified pCSII-EF-MCS (43) for delivery of anti-*HBZ* short hairpin RNAs, and recombinant lentivirus was produced as described in the *Supporting Methods*. The titer of concentrated virus stocks was measured on 293 T cells based on their EGFP expression. Cells were then transfected with concentrated vector stocks at a multiplicity of infection of 10–25 in the presence of polybrene (4 μg/ml, Sigma). Cells were harvested 7 days later, and EGFP expression of transfected cells was analyzed with an EPICS XL Flow Cytometer (Beckman Coulter). When >90% of transfected cells expressed EGFP, cell growth and *HBZ* gene expression were analyzed.

Microarray Analysis. Total RNAs were isolated from Kit 225 cells, which were transfected with a vector expressing the *HBZ* gene, the TTG *HBZ* gene (the first ATG of *HBZ* gene was replaced by TTG), or with a control vector by using TRIzol reagent (Invitrogen) according to the manufacturer's protocol. Total RNAs were then purified by RNeasy (Qiagen). Oligonucleotide microarray analyses (CodeLink, Human 20K I bioarrays, Amersham Pharmacia Biosciences) were performed by Kurabo Industries (Osaka) with the authorization of Amersham Pharmacia Biosciences. A 2.0-fold increase or decrease was considered significant, based on the manufacturer's recommendation.

Luciferase Assay. Jurkat cells were grown in RPMI medium 1640 containing 10% FBS. On day 1, cells were seeded into 6-well plates at 4×10^5 cells per well. After 24 h, cells were transfected with 1 μg per well of luciferase reporter plasmid (WT-Luc) (44), 40 ng per well of pRL-TK (Promega), and pCG-Tax (1 μg) (45), and/or an *HBZ* expression plasmid (0.3 or 1 μg), and/or blank expression vector (to normalize the DNA dose) mixed with Transfectin (Bio-Rad). After 48 h, cells were collected and luciferase activities were measured by using a Dual Luciferase Reporter Assay Kit (Promega).

Generation of Transgenic Mice. *HBZ* cDNA was cloned into the SalI site of the H/M/T-CD4 vector, which was designed for restricted expression of a transgene in $CD4^+$ cells (25). The purified fragment containing the *HBZ* transgene was microinjected into C57BL/6J F1 fertilized eggs. Transgenic founders were screened for integration of transgenes by PCR and mated with C57BL/6J mice to generate transgenic progeny. All animals used in this study were maintained and handled according to protocols approved by Kyoto University.

Cell Proliferation Assay. Proliferation assays of murine cells were carried out in RPMI 1640 medium supplemented with 10% FBS and 2-mercaptoethanol (50 μM). Thymocytes (1×10^6 cells per ml) were stimulated by an immobilized anti-CD3 antibody (4 μg/ml) with or without recombinant IL-2 in flat-bottomed 96-well plates. Thymocyte proliferation was measured by ^{3}H-thymidine uptake after 3 days of incubation. Cell viabilities were assessed by measuring 3-(4,5-dimethylthiazol-2-yl)-2,5-diphenyl tetrazolium bromide dye absorbance (42).

Flow Cytometric Analysis. Cell cycles of *HBZ*-transfected and control Kit 225 cells were analyzed after removal of IL-2 (48 h) by using BrdU Flow Kits (Becton Dickinson Pharmingen) according to the manufacturer's instructions. To analyze CD4 and CD8 expression in *HBZ* transgenic mice, cells (5×10^5) were reacted with monoclonal antibodies against murine CD4 (FITC-labeled, Immunotech) and CD8 (phycoerythrin-labeled, Immu-

notech), according to the manufacturer's instructions, and analyzed with an EPICS XL Flow Cytometer (Beckman Coulter).

Statistical Analyses. Statistical analyses were performed by using the unpaired Student *t* test.

We thank S. Yonehara, M. Ohno, H. Sakano, and H. Mitsuya for helpful discussions; A. Koito (Kumamoto University, Kumamoto, Japan) for providing the H/M/T-CD4 vector; S. Yamada (Akita University, Akita, Japan) for help in generating transgenic mice; H. Miyoshi (The Institute of Physical and Chemical Research, Tsukuba Institute, Tsukuba, Japan) for the gift of pCSII-EF-MCS vector; J. Fujisawa (Kansai Medical University, Moriguchi, Japan) for the gift of pWT-Luc; T. Hori (Kyoto University) for providing the Kit 225 cell line; and Elise Lamar for proofreading the manuscript. This study was supported by a Grant-in-aid for Scientific Research from the Ministry of Education, Science, Sports, and Culture of Japan.

1. Gallo, R. C. (2002) *Immunol. Rev.* **185,** 236–265.
2. Yoshida, M. (2001) *Annu. Rev. Immunol.* **19,** 475–496.
3. Franchini, G., Fukumoto, R. & Fullen, J. R. (2003) *Int. J. Hematol.* **78,** 280–296.
4. Poiesz, B. J., Ruscetti, F. W., Gazdar, A. F., Bunn, P. A., Minna, J. D. & Gallo, R. C. (1980) *Proc. Natl. Acad. Sci. USA* **77,** 7415–7419.
5. Gallo, R. C. (2005) *Retrovirology* **2,** 17.
6. Takatsuki, K. (2005) *Retrovirology* **2,** 16.
7. Igakura, T., Stinchcombe, J. C., Goon, P. K., Taylor, G. P., Weber, J. N., Griffiths, G. M., Tanaka, Y., Osame, M. & Bangham, C. R. (2003) *Science* **299,** 1713–1716.
8. Jeang, K. T., Giam, C. Z., Majone, F. & Aboud, M. (2004) *J. Biol. Chem.* **279,** 31991–31994.
9. Suzuki, T., Uchida-Toita, M. & Yoshida, M. (1999) *Oncogene* **18,** 4137–4143.
10. Etoh, K., Tamiya, S., Yamaguchi, K., Okayama, A., Tsubouchi, H., Ideta, T., Mueller, N., Takatsuki, K. & Matsuoka, M. (1997) *Cancer Res.* **57,** 4862–4867.
11. Cavrois, M., Leclercq, I., Gout, O., Gessain, A., Wain-Hobson, S. & Wattel, E. (1998) *Oncogene* **17,** 77–82.
12. Matsuoka, M. (2005) *Retrovirology* **2,** 27.
13. Furukawa, Y., Kubota, R., Tara, M., Izumo, S. & Osame, M. (2001) *Blood* **97,** 987–993.
14. Koiwa, T., Hamano-Usami, A., Ishida, T., Okayama, A., Yamaguchi, K., Kamihira, S. & Watanabe, T. (2002) *J. Virol.* **76,** 9389–9397.
15. Takeda, S., Maeda, M., Morikawa, S., Taniguchi, Y., Yasunaga, J., Nosaka, K., Tanaka, Y. & Matsuoka, M. (2004) *Int. J. Cancer* **109,** 559–567.
16. Tamiya, S., Matsuoka, M., Etoh, K., Watanabe, T., Kamihira, S., Yamaguchi, K. & Takatsuki, K. (1996) *Blood* **88,** 3065–3073.
17. Bangham, C. R. (2003) *Int. J. Hematol.* **78,** 297–303.
18. Taniguchi, Y., Nosaka, K., Yasunaga, J. I., Maeda, M., Mueller, N., Okayama, A. & Matsuoka, M. (2005) *Retrovirology* **2,** 64.
19. Larocca, D., Chao, L. A., Seto, M. H. & Brunck, T. K. (1989) *Biochem. Biophys. Res. Commun.* **163,** 1006–1013.
20. Gaudray, G., Gachon, F., Basbous, J., Biard-Piechaczyk, M., Devaux, C. & Mesnard, J. M. (2002) *J. Virol.* **76,** 12813–12822.
21. Basbous, J., Arpin, C., Gaudray, G., Piechaczyk, M., Devaux, C. & Mesnard, J. M. (2003) *J. Biol. Chem.* **278,** 43620–43627.
22. Seiki, M., Hattori, S., Hirayama, Y. & Yoshida, M. (1983) *Proc. Natl. Acad. Sci. USA* **80,** 3618–3622.
23. Hori, T., Uchiyama, T., Tsudo, M., Umadome, H., Ohno, H., Fukuhara, S., Kita, K. & Uchino, H. (1987) *Blood* **70,** 1069–1072.
24. Zuker, M. (2003) *Nucleic Acids Res.* **31,** 3406–3415.
25. Sawada, S., Gowrishankar, K., Kitamura, R., Suzuki, M., Suzuki, G., Tahara, S. & Koito, A. (1998) *J. Exp. Med.* **187,** 1439–1449.
26. Akagi, T., Ono, H. & Shimotohno, K. (1995) *Blood* **86,** 4243–4249.
27. Nevins, J. R. (1998) *Cell Growth Differ.* **9,** 585–593.
28. Weinberg, R. A. (1996) *Cell* **85,** 457–459.
29. Nevins, J. R. (2001) *Hum. Mol. Genet.* **10,** 699–703.
30. Pierce, A. M., Gimenez-Conti, I. B., Schneider-Broussard, R., Martinez, L. A., Conti, C. J. & Johnson, D. G. (1998) *Proc. Natl. Acad. Sci. USA* **95,** 8858–8863.
31. Iwanaga, R., Ohtani, K., Hayashi, T. & Nakamura, M. (2001) *Oncogene* **20,** 2055–2067.
32. Kannagi, M., Harada, S., Maruyama, I., Inoko, H., Igarashi, H., Kuwashima, G., Sato, S., Morita, M., Kidokoro, M., Sugimoto, M., *et al.* (1991) *Int. Immunol.* **3,** 761–767.
33. Inoue, J., Yoshida, M. & Seiki, M. (1987) *Proc. Natl. Acad. Sci. USA* **84,** 3653–3657.
34. Nicot, C., Dundr, M., Johnson, J. M., Fullen, J. R., Alonzo, N., Fukumoto, R., Princler, G. L., Derse, D., Misteli, T. & Franchini, G. (2004) *Nat. Med.* **10,** 197–201.
35. He, L. & Hannon, G. J. (2004) *Nat. Rev. Genet.* **5,** 522–531.
36. Pfeffer, S., Zavolan, M., Grasser, F. A., Chien, M., Russo, J. J., Ju, J., John, B., Enright, A. J., Marks, D., Sander, C. & Tuschl, T. (2004) *Science* **304,** 734–736.
37. Sullivan, C. S., Grundhoff, A. T., Tevethia, S., Pipas, J. M. & Ganem, D. (2005) *Nature* **435,** 682–686.
38. Omoto, S., Ito, M., Tsutsumi, Y., Ichikawa, Y., Okuyama, H., Brisibe, E. A., Saksena, N. K. & Fujii, Y. R. (2004) *Retrovirology* **1,** 44.
39. Bennasser, Y., Le, S. Y., Benkirane, M. & Jeang, K. T. (2005) *Immunity* **22,** 607–619.
40. Iwakiri, D., Eizuru, Y., Tokunaga, M. & Takada, K. (2003) *Cancer Res.* **63,** 7062–7067.
41. Yang, L., Aozasa, K., Oshimi, K. & Takada, K. (2004) *Cancer Res.* **64,** 5332–5337.
42. Yoshida, M., Nosaka, K., Yasunaga, J., Nishikata, I., Morishita, K. & Matsuoka, M. (2004) *Blood* **103,** 2753–2760.
43. Bai, Y., Soda, Y., Izawa, K., Tanabe, T., Kang, X., Tojo, A., Hoshino, H., Miyoshi, H., Asano, S. & Tani, K. (2003) *Gene Ther.* **10,** 1446–1457.
44. Fujisawa, J., Toita, M. & Yoshida, M. (1989) *J. Virol.* **63,** 3234–3239.
45. Fujisawa, J., Toita, M., Yoshimura, T. & Yoshida, M. (1991) *J. Virol.* **65,** 4525–4528.

Correction

MEDICAL SCIENCES. For the article "*HTLV-I basic leucine zipper factor* gene mRNA supports proliferation of adult T cell leukemia cells," by Yorifumi Satou, Jun-ichirou Yasunaga, Mika Yoshida, and Masao Matsuoka, which appeared in issue 3, January 17, 2006, of *Proc. Natl. Acad. Sci. USA* (**103,** 720–725; first published January 9, 2006; 10.1073/pnas.0507631103), the authors note that in Fig, 1*A*, the splicing acceptor site should be 7267 and the splicing donor site should be 8667. The corrected figure and its legend appear below. These errors do not affect the conclusions of the article.

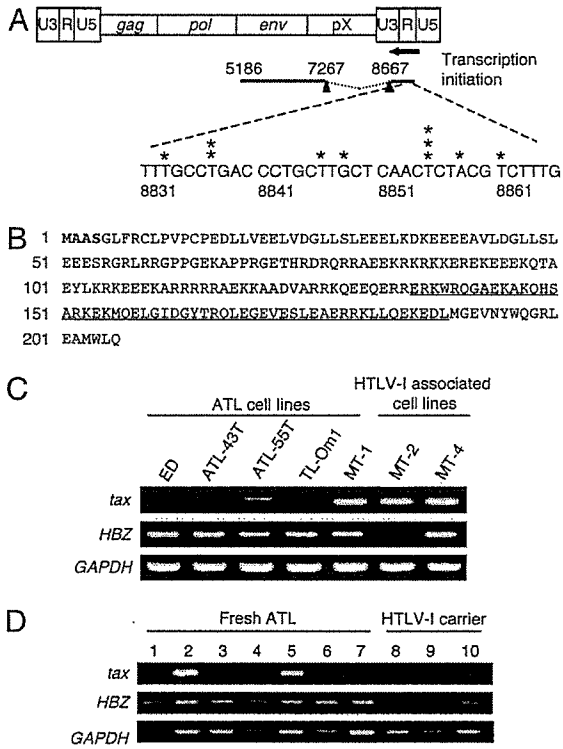

Fig. 1. *HBZ* gene expression in ATL cells. (*A*) 5′ RACE was performed by using total RNA from the ATL cell line ATL-55T. The schema represents the HTLV-I provirus and spliced *HBZ* mRNA. Asterisks show transcription initiation sites identified by 5′ RACE. The 3′ end of the transcript (5186) was identified by 3′ RACE, and polyadenylation signal was found upstream (5206–5211) of this transcript. Nucleic acids are numbered with reference to ATK-1 according to Seiki *et al.* (22). (*B*) Hypothetical amino acid sequence derived from spliced *HBZ*. Amino acids different from the previously reported HBZ are shown in bold type. The basic leucine zipper domain is underlined. (*C*) Expression of *tax* and *HBZ* genes in ATL and HTLV-I-immortalized cell lines analyzed by RT-PCR. (*D*) Expression of *tax* and *HBZ* genes in fresh ATL cells and peripheral blood mononuclear cells from HTLV-I carriers. Lanes: 1–7, fresh ATL cases; 8–10, peripheral blood mononuclear cells from HTLV-I carriers.

www.pnas.org/cgi/doi/10.1073/pnas.0603212103

JOURNAL OF VIROLOGY, Nov. 2006, p. 10683–10691 Vol. 80, No. 21
0022-538X/06/$08.00+0 doi:10.1128/JVI.01009-06

De Novo Human T-Cell Leukemia Virus Type 1 Infection of Human Lymphocytes in NOD-SCID, Common γ-Chain Knockout Mice▽

Paola Miyazato,[1] Jun-ichirou Yasunaga,[1] Yuko Taniguchi,[1] Yoshio Koyanagi,[2] Hiroaki Mitsuya,[3] and Masao Matsuoka[1]*

Laboratory of Virus Immunology[1] and Laboratory of Virus Pathogenesis,[2] Institute for Virus Research, Kyoto University, Kyoto 606-8507, Japan, and Department of Hematology and Department of Infectious Diseases, Graduate School of Medicine, Kumamoto University, Kumamoto 860-8556, Japan[3]

Received 17 May 2006/Accepted 21 August 2006

Human T-cell leukemia virus type 1 (HTLV-1) is the etiologic agent of adult T-cell leukemia, a disease that is triggered after a long latency period. HTLV-1 is known to spread through cell-to-cell contact. In an attempt to study the events in early stages of HTLV-1 infection, we inoculated uninfected human peripheral blood mononuclear cells and the HTLV-1-producing cell line MT-2 into NOD-SCID, common γ-chain knockout mice (human PBMC-NOG mice). HTLV-1 infection was confirmed with the detection of proviral DNA in recovered samples. Both $CD4^+$ and $CD8^+$ T cells were found to harbor the provirus, although the latter population harbored provirus to a lesser extent. Proviral loads increased with time, and inverse PCR analysis revealed the oligoclonal proliferation of infected cells. Although *tax* gene transcription was suppressed in human PBMC-NOG mice, it increased after in vitro culture. This is similar to the phenotype of HTLV-1-infected cells isolated from HTLV-1 carriers. Furthermore, the reverse transcriptase inhibitors azidothymidine and tenofovir blocked primary infection in human PBMC-NOG mice. However, when tenofovir was administered 1 week after infection, the proviral loads did not differ from those of untreated mice, indicating that after initial infection, clonal proliferation of infected cells was predominant over de novo infection of previously uninfected cells. In this study, we demonstrated that the human PBMC-NOG mouse model should be a useful tool in studying the early stages of primary HTLV-1 infection.

Human T-cell leukemia virus type 1 (HTLV-1) was the first retrovirus shown to be related to human diseases (21, 44), including adult T-cell leukemia (ATL) (50, 51, 58) and HTLV-1-associated myelopathy/tropical spastic paraparesis (HAM/TSP) (16, 43). The infectivity of free virions is much lower than that of infected cells: transmission is cell mediated (8). Glucose transporter 1 has been identified as an HTLV-1 receptor (35). After infected cells form virological synapses with uninfected cells, the viral genome is transferred into uninfected cells (23). Hence, a salient feature of HTLV-1 infection is that this virus transmits in a cell-to-cell fashion. After infection, HTLV-1 facilitates cell-to-cell transmission by forcing the proliferation of infected cells via the actions of its accessory genes.

In the early stage of HTLV-1 infection, accessory genes including *p12*, *p30*, *p13*, and *HBZ*, have been reported to be important for in vivo proliferation of infected cells (3, 5, 22, 47). The gene product p12 plays a critical role by releasing calcium from the endoplasmic reticulum to activate nuclear factor of activated T cell-mediated transcription (2). In addition, p12 enhances lymphocyte-associated antigen-1-mediated cell adhesion, which might facilitate cell-to-cell transmission of HTLV-1 (29), and downmodulates the expression of major histocompatibility complex class I antigens (26). p30 has been reported to suppress viral gene transcription by different mechanisms (41). Other functions of p30 have been also demonstrated, such as the enhancement of the transcription of cellular genes associated with cell proliferation (38, 64). In addition, the *tax* gene is believed to play a central role in proliferation of infected cells by its pleiotropic actions (14, 17, 63). On the other hand, Tax-expressing cells are rapidly eliminated in vivo, since the Tax protein is a major target antigen of cytotoxic T lymphocytes (CTLs) (4, 27). In ATL cells, Tax expression has been shown to be suppressed by several mechanisms (52), strongly suggesting that the loss of Tax expression might be advantageous at the stage of leukemia (36). These studies reveal that the host immune system plays an important role in limiting the proliferation of infected cells. During the long latency period that spans decades, this immune pressure selects those clones with enough alterations to become malignant, eventually leading to the development of ATL.

In vivo studies of HTLV-1 infection have been carried out mainly by inoculating virus-producing or HTLV-1-immortalized cell lines into different animal species (32). Rabbits proved to be an effective model for HTLV-1 infection (1, 65). In addition, monkeys and rats have been used to analyze the in vivo proliferation of HTLV-1-infected cells (7, 55). Furthermore, immunodeficient mouse strains were also able to engraft some HTLV-1-immortalized cell lines (13, 24). These animal models are useful for studying the infection or testing therapeutic agents. However, the early steps of primary HTLV-1 infection remain uninvestigated due to the lack of in vivo experiments using human lymphocytes.

The NOD-SCID (nonobese diabetic-severe combined immunodeficiency), common γ-chain knockout (NOG) mouse was shown to be an excellent recipient for transplantation of

* Corresponding author. Mailing address: Laboratory of Virus Immunology, Institute for Virus Research, Kyoto University, Shogoin Kawahara-cho 53, Sakyo-ku, Kyoto 606-8507, Japan. Phone: 81-75-751-4048. Fax: 81-75-751-4049. E-mail: mmatsuok@virus.kyoto-u.ac.jp.

▽ Published ahead of print on 30 August 2006.

human cells due to multiple immune dysfunctions (9, 25, 60). We report here the primary infection of human lymphocytes in this newly developed mouse strain and characterize the infection by measuring proviral load as well as determining the clonality pattern. Furthermore, we tested whether the existing antiretroviral drugs azidothymidine (AZT) and tenofovir blocked primary infection in this mouse model. This small animal model allows us to better understand the mechanism of HTLV-1 infection.

MATERIALS AND METHODS

Cells. Peripheral blood mononuclear cells (PBMC) were isolated from healthy blood donors by Ficoll-Paque Plus (Pharmacia, Uppsala, Sweden) density gradient centrifugation. MT-2, an HTLV-1-producing cell line (61), was used as the source of virus in all the experiments. MT-2 cells were treated with 50 μg/ml of mitomycin C (MMC) (Kyowa, Tokyo, Japan) for 30 min at 37°C in RPMI 1640 supplemented with 10% fetal bovine serum and antibiotics and washed four times with culture medium prior to inoculation into mice. PBMC of 14 healthy donors were used in the experiments. For in vitro cytotoxicity assays, PBMC were stimulated with phytohemagglutinin (PHA) (Sigma, St. Louis, Mo.) prior to use.

Mice. The NOG strain of mice, which was generated by backcross matings of C57BL/6J-γc^{null} mice and NOD/Shi-SCID mice, is homozygous for the SCID mutation and the interleukin 2Rγ allelic mutation. It was previously reported to present multiple immunological dysfunctions that include the absence of T, B, and NK cells and also impaired activity of dendritic cells (25). Mice were purchased from the Central Institute of Experimental Animals (Kanagawa, Japan) and were maintained in microisolator cages under specific-pathogen-free conditions in the animal facility of the Institute for Virus Research, Kyoto University (Kyoto, Japan). Mice were 6 to 7 weeks old at the time of the human PBMC transfer.

Transplantation of human PBMC in NOG mice and infection with HTLV-1. A total of 10^7 human PBMC were injected intraperitoneally into each mouse, producing chimeric mice, which we will refer to as hu-PBMC-NOG mice. Three days later, the mice were inoculated intraperitoneally with MMC-treated MT-2 cells (10^3 or 10^4 cells/mouse). Spleens and cells obtained from peritoneal lavage were harvested two or four weeks after injection of MT-2 cells. Human mononuclear cells were isolated by Ficoll-Paque Plus (Pharmacia) density gradient centrifugation prior to analysis. The experimental protocol was approved by the Ethics Review Committee for Animal Experimentation of Institute for Virus Research, Kyoto University. In each independent experiment, PBMC from a single donor were used.

Quantification of HTLV-1 proviral load. Genomic DNA was obtained from the samples by standard proteinase K treatment. To quantify the proviral load, we performed a real-time PCR as we described previously (62). The primers for exon 3 of the HTLV-1 *tax* gene were 5′-GAAGACTGTTTGCCCACCACC-3′ and 5′-TGAGGGTTGAGTGGAACGGA-3′, and the probe was 5′-CACCCG TCACGCTAACAGCCTGGCAA-3′. Genomic DNA (500 ng) was used for real-time PCR in a 50-μl reaction solution prepared with TaqMan Universal PCR master mix (Applied Biosystems, Foster City, CA). The amplification conditions were 50°C for 2 min, 95°C for 10 min, and then 40 cycles of 15 s at 95°C followed by 60 s at 60°C. All experiments were performed and analyzed using the ABI PRISM 7700 sequence detection system (Applied Biosystems). To measure cell equivalents in the input DNA, the recombination activating gene 1 (*RAG-1*) coding sequence in each sample was also quantified by real-time PCR. The sequences of the primers for *RAG-1* exon 2 detection were 5′-CCCACCTTGG GACTCAGTTCT-3′ and 5′-CACCCGGAACAGCTTAAATTTC-3′, and the probe was 5′-CCCCAGATGAAATTCAGCACCCACATA-3′. Amplification conditions were the same as those for *tax*. The probes were labeled with fluorescent 6-carboxyfluorescein (reporter) at the 5′ end and fluorescent 6-carboxytetramethylrhodamine (quencher) at the 3′ end. All samples were analyzed in duplicate. The DNA of freshly purified ATL cells, which harbor one copy of the HTLV-1 provirus, was used as positive control, and its proviral load was given the value of 100% when used as point of comparison.

IL-PCR. In order to study the clonality of HTLV-1 infected cells in hu-PBMC-NOG mice, we performed an inverse long PCR (IL-PCR) (10). Briefly, 1 μg of genomic DNA was first digested with EcoRI (TOYOBO, Osaka, Japan) and then self-ligated with T4 DNA ligase (TOYOBO) overnight at 4°C. Circularized DNA was then linearized with MluI (TOYOBO) to prevent amplification of the proviral sequence itself. The resulting DNA was used as template for IL-PCR, performed with LA *Taq* HS (Takara Bio Inc., Otsu, Japan). Amplification conditions were as follows: 94°C for 2 min; 40 cycles of 94°C for 30 s and 64°C for 10 min; and a final extension at 72°C for 15 min, using a Robocycler thermal cycler (Stratagene, La Jolla, CA). PCR products were electrophoresed in a 1% agarose gel and were then visualized via ethidium bromide staining.

Flow cytometric analysis. T-cell subsets of splenocytes were analyzed by flow cytometry (EPICS Coulter-Beckman, Fullerton, CA). Briefly, 10^6 cells were double stained with anti-human CD4-PC5 (Immunotech, Marseille, France) or anti-human CD8-PC5 (Immunotech) and anti-human CD45RO-fluorescein isothiocyanate (FITC) (Immunotech) or anti-human CD25-R-phycoerythrin (Caltag Laboratories, Burlingame, CA). They were also stained with anti-human CD45-FITC (Immunotech) and anti-mouse CD45-phycoerythrin (Immunotech) to assess the predominance of human cells in the recovered splenocytes. Cells were also stained with anti-human CD3-FITC (Sigma) and anti-human CD19-FITC (BD Biosciences, San Jose, CA).

Purification using magnetic beads. $CD4^+$ and $CD8^+$ T cells were isolated from 10^7 whole splenocytes by using BD IMag magnetic beads (BD Biosciences) according to the manufacturer's instructions. Positive selection of these T-cell subpopulations was performed using anti-human CD4- and anti-human CD8-conjugated magnetic particles.

Reverse transcriptase PCR (RT-PCR). RNA was extracted from splenic cells at the time of sacrifice and after 24 h of in vitro culture by using TRIzol reagent (Invitrogen, Carlsbad, CA) according to manufacturer's instructions. One microgram of total RNA was reverse transcribed by using the RNA LA PCR kit (using avian myeloblastosis virus) version 1.1 (Takara) using random primers. One microliter of cDNA was used as the PCR template. The following primers were used: 5′-CCGGCGCTGCTCTCATCCCGG-3′ and 5′-GGCCGAACATA GTCCCCCAGAG-3′ for *tax* and 5′-GCAGGGGGGAGCCAAAAGGG-3′ and 5′-TGCCAGCCCCAGCGTCAAAG-3′ for the GAPDH (glyceraldehyde-3-phosphate dehydrogenase) gene. The amplification conditions were as follows: 95°C for 2 min; 40 cycles of 95°C for 30 s, 62°C for 30 s, and 72°C for 30 s; and a final extension at 72°C for 2 min (for *tax*); 95°C for 3 min; 22 cycles of 95°C for 20 s, 57°C for 30 s, and 72°C for 1 min; and a final extension at 72°C for 7 min (for the GAPDH gene) in a thermal cycler (ASTEC, Fukuoka, Japan). PCR products were electrophoresed in a 2% agarose gel and visualized via ethidium bromide staining. For real-time PCR, an ABI PRISM 7500 sequence detector (Applied Biosystems) was used. Data were analyzed by a comparative cycle threshold method. The level of *tax* mRNA in the MT-1 cell line was used as a positive control and was assigned a value of 100 arbitrary units.

Sodium bisulfite treatment of genomic DNA. Sodium bisulfite treatment was performed as previously described (54). Briefly, 1 μg of genomic DNA was denatured in 0.3 N NaOH at 37°C for 15 min, and 1 μg of salmon sperm DNA was added to each sample to act as a carrier. Sodium bisulfite (pH 5.0) and hydroquinone were added to each sample to final concentrations of 3 M and 0.05 mM, respectively, and the reaction mixture was incubated at 55°C for 16 h. Samples were then desalted using the Wizard DNA cleanup system (Promega, Madison, WI). Finally, samples were desulfonated in 0.3 N NaOH at 37°C for 15 min.

COBRA. For a combined bisulfite restriction analysis (COBRA) (59), different regions of the HTLV-1 provirus were amplified from sodium bisulfite-treated genomic DNA (54). The nested PCRs were performed using FastStart *Taq* DNA polymerase (Roche, Mannheim, Germany) under the following conditions: 95°C for 5 min; 40 cycles of 30 s at 95°C, 30 s at each annealing temperature, and 30 s at 72°C; and 2 min at 72°C for a final extension. The sequences of the primers used, and their annealing temperatures are as described previously (54). The PCR products were digested for at least 4 h with TaqI restriction enzyme, which resulted in a single recognition site within each product. The digested PCR products were separated in a 3% Nusieve 3:1 agarose (BMA, Rockland, ME) gel. The intensity of each fragment was determined by using a densitograph (version 4.0; ATTO, Tokyo, Japan).

Treatment with reverse transcriptase inhibitors in mice. hu-PBMC-NOG mice were inoculated with 10^3 MMC-treated MT-2 cells 3 days after transfer of human PBMC and were then divided into three groups for treatment, with AZT (240 mg/kg of body weight/day) (Nacalai Tesque, Kyoto, Japan), tenofovir (130 mg/kg/day) (kindly provided by Gilead Sciences Inc., CA), or phosphate-buffered saline (PBS). They were treated immediately after MT-2 inoculation for 12 days and then sacrificed to recover spleens and cells from peritoneal lavage for analysis. Tenofovir and AZT were administered intraperitoneally 2 and 3 times a day, respectively. The control group was injected twice a day with PBS. In another experiment, two groups of mice received treatment with AZT for 7 days or tenofovir for 12 days beginning one week after infection with 10^4 or 10^3 MT-2 cells/mouse, respectively. Each independent experiment was performed using the PBMC from a single donor.

TABLE 1. Proviral load of mice inoculated with different numbers of MT-2 cells[a]

Donor	No. of MT-2 cells in inoculation	Proviral load (%)	
		Lavage specimen	Spleen
A	10^2	0.0	0.0
	10^3	0.3	0.0
	10^4	4.2	1.2
B	10^2	1.1	0.2
	10^3	2.5	0.4
	10^4	0.9	2.0
C	10^6	83.2	26.5
	10^6	97.9	71.7
	10^6	90.4	53.4

[a] Proviral loads of cells recovered from the peritoneal cavity and spleens 2 (for donors A and B) or 3 (for donor C) weeks after inoculation of the specified numbers of MT-2 cells are shown for mice initially receiving PBMC of three different human donors.

MTT assay. The inhibitory effects of tenofovir and AZT on cell growth were assessed by MTT [3-(4,5-dimethylthiazol-2-yl)-2,5-diphenyl tetrazolium bromide] assay, which is based on the reduction of MTT by metabolically active cells to a blue formazan that can be measured spectrophotometrically. PBMC of three different donors (10^5 cells/well) were cultured in the presence or absence of the RT inhibitors (serial 10-fold dilutions from 5 mM to 0.05 μM) and 20 U/ml of interleukin 2 (kindly provided by Shionogi & Co., Ltd., Osaka, Japan) in a 96-well plate for three days. Twenty microliters of MTT solution (7.5 mg/ml) was added to each well, and the plate was incubated at 37°C for 5 h. One hundred twenty microliters of the medium was removed and 100 μl of acidified isopropanol containing 4% (vol/vol) of Triton X was added to each well to dissolve the formazan crystals. Viability relative to the untreated control was determined. Drug concentrations which inhibited cell growth by 50% (i.e., 50% cytotoxic concentrations) were also calculated from these data. All assays were performed in quadruplicate.

RESULTS

De novo HTLV-1 infection of human PBMC in NOG mice. In order to establish an in vivo model for primary HTLV-1 infection of human lymphocytes, we chose NOG mice as recipients because they were proven to engraft human cells with high efficiency (25, 60). We first determined the number of MT-2 cells necessary to achieve infection in this new mouse model. We inoculated human PBMC of two different donors intraperitoneally and, three days later, injected different numbers of MMC-treated MT-2 cells, since HTLV-1 transmits efficiently only in a cell-to-cell fashion (23, 45, 61). Two weeks later, cells were recovered from the peritoneal cavity and the spleen of each mouse and proviral load was determined by real-time PCR (Table 1). A total of 10^3 MT-2 cells was enough to produce a detectable level of proviral load in both groups of NOG mice. Taking these results into account, we decided to use 10^3 or 10^4 MT-2 cells in the following experiments. Another group of mice was inoculated with 10^6 MT-2 cells and sacrificed 3 weeks later, which led to significantly increased proviral loads (Table 1).

To check the effects of different donor sources on proviral load, we inoculated PBMC from six healthy donors into NOG mice and found that the proportions of subpopulations in T and B lymphocytes did not influence proviral loads at 2 weeks after inoculation of MT-2 cells, and the proviral loads, even in mice inoculated with cells from the same donor, were variable, especially in cells from lavages (Table 2). Regarding provirus loads in spleen cells, variations were not so remarkable. In the following experiments, we used PBMC from a single donor in each experiment.

TABLE 2. Phenotypes of donor PBMC and proviral loads of cells recovered from infected hu-PBMC-NOG mice[a]

Donor	Surface markers of donor PBMC (%)[b]				Proviral load (%)[c]	
	CD3	CD4	CD8	CD19	Lavage specimen	Spleen
D	69.7	61.8	18.7	12.2	3.7	0.6
					34.0	1.4
					2.8	0.5
E	84.7	53.4	33.9	3.0	0.6	0.1
					12.6	1.0
					11.6	0.8
F	67.0	48.0	31.9	2.8	0.2	0.0
					2.7	0.2
					0.6	0.1
G	74.9	43.9	37.7	1.3	7.4	0.2
					2.8	0.6
H	80.0	62.8	18.0	1.2	2.4	0.2
					0.4	0.0
I	ND	ND	ND	ND	20.5	2.5
					0.1	0.3

[a] PBMC from the indicated donors were transferred into NOG mice, and these were sacrificed 2 weeks after inoculation of 10^4 MMC-treated MT-2 cells.
[b] The percentage of cells positive for the specified markers before transfer into mice is shown for each donor.
[c] The proviral loads of human cells recovered from peritoneal lavage and spleens of the different mice are shown as percentages, calculated as described in Materials and Methods. ND, not determined.

In order to characterize the primary infection with HTLV-1, we inoculated a group of mice with 10^4 MT-2 cells after the transfer of PBMC and analyzed them in two groups at 2 and 4 weeks postinfection (p.i.). To assess the proportions of human cells in the studied specimens, we stained recovered cells with anti-mouse-CD45 and anti-human-CD45 antibodies and analyzed them by flow cytometry. Human cells accounted for at least 85% of the recovered splenocytes two weeks after the transfer and reached more than 94% in the group analyzed at 4 weeks p.i. (data not shown). The total number of recovered human lymphocytes was much larger than the number initially inoculated. Two weeks after the transfer of 10^7 human PBMC, we were able to recover $(7.7 \pm 3.4) \times 10^7$ human cells from the spleen of MT-2-inoculated mice and $(8.1 \pm 2.7) \times 10^7$ human cells from the spleen of the control group. These results demonstrate both migration from the peritoneal cavity to the spleen and in vivo cell expansion. There was no significant difference between the numbers of recovered splenocytes from the MT-2-inoculated and the uninoculated control groups, indicating that the cell proliferation was probably due to xenogeneic stimulation. This suggests that, in the early stages, many cells are stimulated to proliferate in the NOG mouse environment regardless of HTLV-1 infection.

In order to confirm HTLV-1 infection, we amplified a frag-

TABLE 3. Proviral load of in vivo infected cells[a]

Mouse	Proviral load (%)	
	Lavage specimen	Spleen
2-wk group		
2W-1	3.7	0.6
2W-2	34.0	1.4
2W-3	2.8	0.5
4-wk group		
4W-1	33.6	14.1
4W-2	48.1	12.9

[a] The percentages of the proviral load, calculated by comparison with a control DNA as described in Materials and Methods are shown for cells recovered from abdominal lavage and cells isolated from spleens of MT-2-inoculated hu-PBMC-NOG mice.

TABLE 4. Proviral load in $CD4^+$ and $CD8^+$ T cells[a]

Mouse	Proviral load (%)	
	$CD4^+$	$CD8^+$
2-wk group		
2W-1	0.6	0.7
2W-2	4.5	1.1
2W-3	1.2	0.4
4-wk group		
4W-1	14.9	7.8
4W-2	19.9	13.6

[a] Human $CD4^+$ and $CD8^+$ T cells were purified from 10^7 splenocytes of mice sacrificed at 2 or 4 weeks p.i. with the use of magnetic beads. Proviral load was determined by real-time PCR as described in Materials and Methods.

ment of the HTLV-1 pX region by using PCR, and proviral DNA was detected in the cells recovered from the MT-2-inoculated groups of hu-PBMC-NOG mice (data not shown). These PCR products were not derived from contamination of cellular DNA of MT-2 cells, since a PCR specific for one of HTLV-1 integration sites in MT-2 did not detect the provirus (data not shown). Splenocytes tended to have a lower proviral load than cells recovered from the peritoneal cavity. However, the proviral load in the 4-week group was generally greater than that from the 2-week group, suggesting the continuous proliferation of infected cells and propagation of the virus in this mouse model (Table 3).

Significant increase in the memory $CD4^+$ T-cell population after HTLV-1 infection. Although HTLV-1 is known to infect many types of cells in vivo (31), the majority of HTLV-1-infected cells are $CD4^+$ memory T cells (46, 62). To determine the effect of HTLV-1 infection on subpopulations of lymphocytes, we studied the expression of surface molecules by flow cytometry. Two weeks after infection, there was a significant increase in the cell population expressing CD4 and CD45RO molecules in the infected group compared to that in the control group (Fig. 1), suggesting that in the infected group of mice, memory $CD4^+$ T cells proliferated. This finding is consistent with observations with HTLV-1 carriers (62). The proviral loads in $CD4^+$ and $CD8^+$ splenic T cells were determined by real-time PCR (Table 4). As previously reported for HTLV-1 carriers, $CD8^+$ T cells were also found to contain the provirus, but to a lesser extent than $CD4^+$ T cells (39, 62). Nevertheless, proviral load tended to increase with time in both subpopulations of T cells (Table 4).

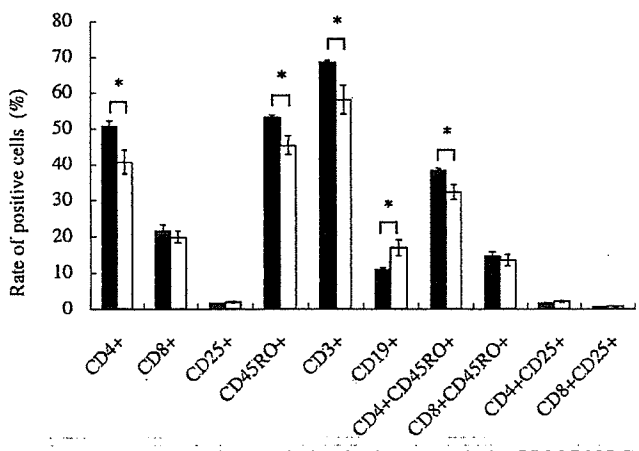

FIG. 1. Surface marker analysis of splenocytes in hu-PBMC-NOG mice. Splenocytes were isolated from hu-PBMC-NOG mice with or without HTLV-1 infection, and their surface markers were analyzed by flow cytometry. Splenocytes were recovered at 2 weeks p.i. The percentages of cells positive for various surface molecules are shown for MT-2-inoculated hu-PBMC-NOG mice (black bars) and uninfected controls (open bars). Values are means ± standard deviations from groups of three mice. *, $P < 0.05$ (Student's t test).

Polyclonal proliferation of HTLV-1-infected cells. In HTLV-1 carriers, polyclonal proliferation of HTLV-1 infected cells has been detected (10). Therefore, the clonality of HTLV-1-infected cells in hu-PBMC-NOG mice was analyzed by IL-PCR. We analyzed the same DNA samples in triplicate. When the same bands are detected in all three reactions, it means that the number of such clones is high. On the other hand, the stochastic results suggest that these clones are minor in vivo. As shown in Fig. 2, multiple bands were detected by IL-PCR at the 2-week time point, indicating an early polyclonal proliferation. At the 4-week time point, the number of bands increased, as did the intensity of bands corresponding to major clones, suggesting that both the numbers of clones and cell numbers of major clones increased (Fig. 2). We further confirmed the presence of different clones in the same mouse by determining the integration sites of the provirus in the human cells (data not shown).

Profile of proviral DNA methylation in primary HTLV-1 infection. Proviral DNA methylation appears to begin at the internal sequences, such as the *gag*, *pol*, and *env* regions (54), and accumulates in vivo. DNA methylation is thought to disturb viral gene transcription when the 5′ long terminal repeat (LTR) is methylated by inhibiting the binding of transcriptional factors (6). We analyzed the DNA methylation status of the proviral DNA in the cells recovered from the mice (Fig. 3). In the 2-week group, none of the three samples tested presented methylation in the *gag*, *pol*, or 5′ LTR regions. However, in the cells recovered from two mice after 4 weeks, the *gag* regions from both mice were partially methylated, and the *pol* region from one of the two mice was methylated. These results coincide with our previous findings that CpG motifs within the proviral sequence of HTLV-1 are methylated in a progressive manner, starting from internal regions and then spreading to the 5′ and 3′ ends of the provirus (54).

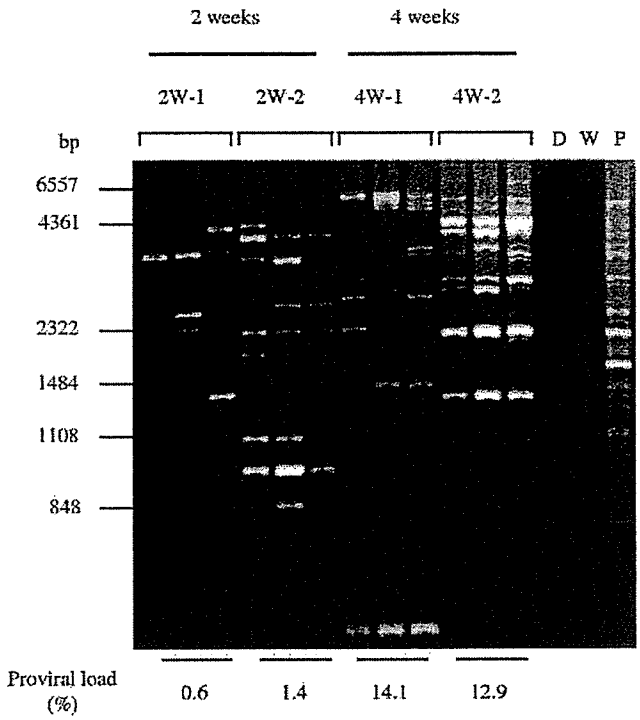

FIG. 2. Polyclonal proliferation of HTLV-1-infected cells in the spleens of hu-PBMC-NOG mice (2W-1, 2W-2, 4W-1, and 4W-2). Genomic DNA was isolated from recovered splenocytes and analyzed by IL-PCR as described in Materials and Methods. IL-PCR was performed in triplicate for each DNA sample. Genomic DNA was recovered from splenocytes at 2 or 4 weeks after injection of MT-2 cells. D, DNA of donor PBMC before inoculation; W, water; P, positive control (DNA from PBMC of an HTLV-1 carrier). In addition, proviral load was quantified by real-time PCR as described in Materials and Methods and is shown as a relative percentage.

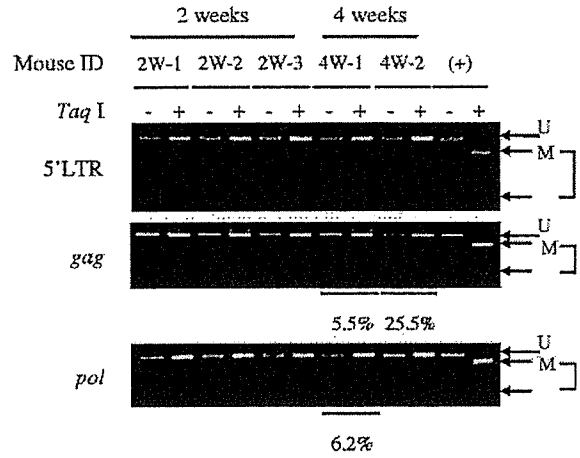

FIG. 3. DNA methylation of HTLV-1 provirus. hu-PBMC-NOG mice were sacrificed 2 or 4 weeks after inoculation of MT-2 cells, and DNA methylation in the 5′ LTR, *gag*, and *pol* regions was studied by a COBRA assay. (+), positive control; U, intact fragment (unmethylated CpG); M, digested fragments (methylated CpG). Percentages of DNA methylation were calculated by densitography according to the following formula (with the variables as described above): [M/(U + M)] × 100.

Suppression of *tax* gene transcription in the NOG mouse model. The viral protein Tax is believed to play an important role in the proliferation of infected cells due to its pleiotropic functions (63). However, its expression in vivo has not been detected in most ATL patients (52). When ATL cells are transferred to culture ex vivo, Tax expression can be recovered (21, 30, 57). Viral gene transcription is also suppressed in PBMC of HAM/TSP patients, as well as asymptomatic HTLV-1 carriers (19, 28). We performed an RT-PCR in order to detect *tax* mRNA in the spleens of infected hu-PBMC-NOG mice sacrificed 2 weeks p.i. (Fig. 4). Transcripts of the *tax* gene were undetectable in two of the three mice when cells were recovered, while the remaining one showed a low level of expression. In all three cases, there was an increase of *tax* gene transcription after 24 h of culture in vitro, even without changes in the proviral load (Fig. 4). Since this phenomenon occurs even in hu-PBMC-NOG mice, a factor(s) other than the host immune system must be involved in the suppression of *tax* gene transcription in vivo.

Effect of antiretroviral agents on HTLV-1 infection. It is well known that HTLV-1 is transmitted through sexual intercourse (49), breast feeding (48), and blood transfusions (42), and for transmission, cell-to-cell contact is thought to be essential. Due to the low capacity of cell-free virus to infect (8, 11), accidental exposures were not thought to confer a high risk of infection, and no prophylactic therapy has been considered. However, the prevalence of HTLV-1 carriers among drug abusers shows that we do need to develop strategies to prevent viral transmission. A previous in vitro study reported that AZT was able to inhibit new HTLV-1 infection of human lymphocytes (37). In addition, it has been reported that tenofovir efficiently inhibited the reverse transcriptase activity of HTLV-1 (20). In order to assess whether a preventive antiretroviral treatment would prove useful in cases of accidental HTLV-1 exposure, we treated hu-PBMC-NOG mice with two reverse transcriptase inhibitors, AZT and tenofovir. The treatment started as soon as MT-2 cells were injected and continued for 12 days. Proviral DNA was undetectable by real-time PCR in the groups of mice treated with AZT or tenofovir (Table 5). Mice seemed to tolerate the treatment without evident signs of toxicity. In the cases where weight loss was seen, it did not exceed 6% of the weight at the time treatment was started (data not shown). However, the number of human cells recovered from spleens of mice receiving AZT treatment was lower than those of the other two groups (Table 5), which indicates that this drug might be also interfering in the proliferation of transferred PBMC. In in vitro assays, we analyzed the cytotoxic effects of AZT and tenofovir on PHA-stimulated human PBMC derived from three different donors. We found that, in a range of concentrations from 5 mM to 0.05 μM, AZT was more toxic than tenofovir when used in incubations for 3 days (Fig. 5). The 50% cytotoxic concentration of AZT was 0.297 ± 0.169 mM, while that of tenofovir was higher than 5 mM. These results indicate that the cytotoxic effect of AZT contributes to suppression of the number of transferred human lymphocytes in our mouse in addition to inhibition of reverse transcriptase.

Clonal expansion of infected cells takes place even in the early stages of primary HTLV-1 infection. It remains undeter-

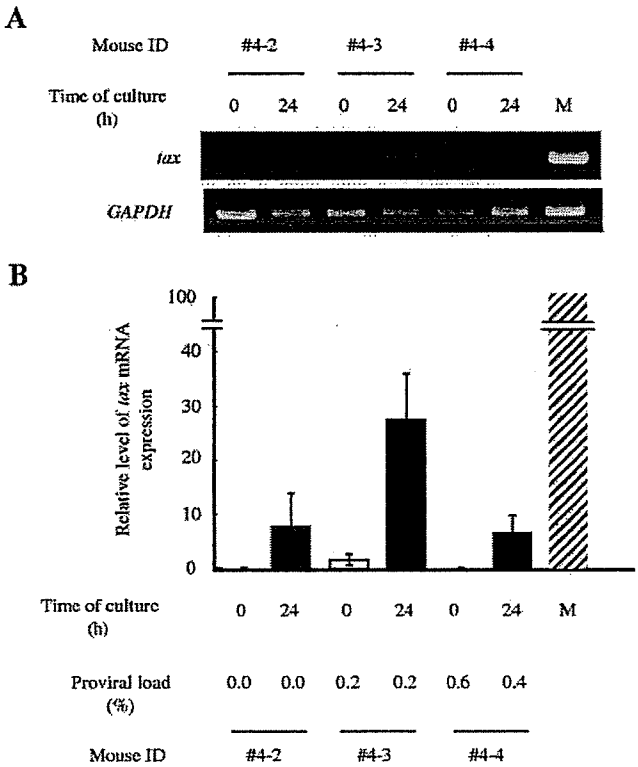

FIG. 4. Transcription of the *tax* gene increases after in vitro culture. Splenocytes of hu-PBMC-NOG mice inoculated with 10^4 MT-2 cells were recovered 2 weeks after infection. Transcription of the *tax* gene was quantified by semiquantitative PCR (A) or real-time PCR (B) at recovery and after 24 h of in vitro culture. Proviral loads for the same samples were also measured by real-time PCR. M, MT-1 cells; ID, identification number.

mined whether clonal proliferation or internal continuous contagion contributes to the increase of HTLV-1-infected cells. To answer this question, hu-PBMC-NOG mice infected with MT-2 cells were treated with tenofovir beginning 1 week after infection. Tenofovir treatment made no significant difference in HTLV-1 proviral load (Table 6), suggesting that clonal proliferation is predominant after HTLV-1 infection. The provirus loads of AZT-treated mice were lower than those of untreated mice, suggesting that the cytotoxic effect of AZT suppressed the provirus loads, as shown in Table 6.

DISCUSSION

Human immunodeficiency virus type 1 vigorously generates progeny virions through the action of its accessory genes, and the resulting free virions play an important role in its transmission, in addition to cell-to-cell transmission. In contrast, for HTLV-1, the efficiency of transmission by free virions is much lower than that via cell-to-cell contact (8), suggesting that HTLV-1 transmits primarily through the latter mechanism. To facilitate such transmission, instead of producing virions, HTLV-1 increases the number of infected cells by the actions of its accessory genes (17, 63). The finding that mother-to-infant transmission was more frequent in mothers with higher proviral loads indicates that such an increase in the number of

TABLE 5. RT inhibitors AZT and tenofovir inhibit de novo infection by HTLV-1[a]

Condition or treatment	Mouse	Proviral load (%)		Cell count (10^6)
		Lavage specimen	Spleen	
Untreated	C1	4.2	1.1	1.6
	C2	0.7	0.0	12.5
	C3	0.0	0.0	19.0
	C4	5.9	0.6	6.0
	C5	0.1	0.1	4.8
Tenofovir	T1	0.0	0.0	5.2
	T2	0.0	0.0	9.2
	T3	0.0	0.0	1.7
	T4	0.0	0.0	8.8
	T5	0.0	0.0	4.0
AZT	A1	0.0	0.0	2.6
	A2	0.0	0.0	3.6
	A3	0.0	0.0	4.5
	A4	0.0	0.0	2.2
	A5	0.0	0.0	2.3

[a] After human PBMC transfer and MT-2 inoculation (10^3 cells/mouse), mice were immediately subjected to antiretroviral therapy with AZT or tenofovir for 12 days. The control group was injected with PBS instead. Proviral loads were determined in cells recovered from the abdominal cavity and spleens. The total numbers of cells recovered from spleens are also shown.

infected cells facilitates the transmission of HTLV-1 (33). In vivo studies using animal models show that the early stage of HTLV-1 infection is controlled by accessory genes, including *p12*, *p13*, *p30*, and *HBZ* genes (3, 5, 22, 47). Thus, although in vivo studies using animal models revealed the importance of accessory genes in replication of HTLV-1 and proliferation of infected cells, the events in the early stages of in vivo transmission in human lymphocytes have not been studied yet due to the lack of an appropriate animal model. Since the metabolisms of nucleosides are quite different among animal species, it is critical to study the effect of reverse transcriptase inhibitors on HTLV-1 in human lymphocytes.

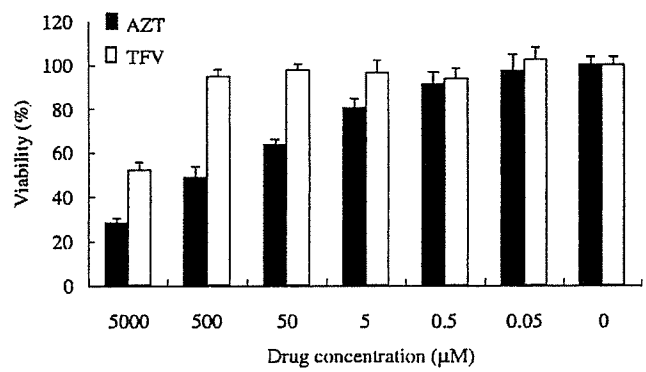

FIG. 5. Cytotoxic effects of tenofovir (TFV) and AZT in vitro. Human PBMC were stimulated with PHA for 3 days. Cells were then cultured in medium alone or medium containing the specified concentration of the indicated drug for another three days, at a density of 10^5 cells/well, in a 96-well plate. Viability was assessed by MTT assay as described in Materials and Methods. The results show the means ± standard deviations of quadruplicate measurements made in one of three representative experiments.

TABLE 6. Proviral load after treatment with tenofovir or AZT beginning one week after infection[a]

Condition or treatment	Mouse	Proviral load (%)	
		Lavage specimen	Spleen
Untreated	U11	7.4	1.7
	U12	0.1	0.0
	U13	15.4	1.9
	U14	3.8	0.7
Tenofovir	T11	0.0	0.0
	T12	0.2	0.0
	T13	15.9	1.8
	T14	14.5	2.6
Untreated	U21	0.6	0.1
	U22	ND	3.0
	U23	12.6	1.0
	U24	11.6	0.8
AZT	A21	0.0	0.0
	A22	ND	0.6
	A23	2.5	0.0
	A24	0.1	0.0

[a] After human PBMC transfer and MT-2 inoculation (10^3 cells/mouse for the tenofovir group, and 10^4 cells/mouse for the AZT group), mice were left for one week before starting treatment with tenofovir or AZT. The control groups were injected with PBS instead of the drugs. Mice were sacrificed 7 or 12 days after treatment with AZT or tenofovir, respectively. Splenocytes, as well as cells from the abdominal cavity, were recovered for analysis as described in Materials and Methods. ND, not determined.

It is widely accepted that the HTLV-1 virion per se is poorly infectious (8, 11) and that cell-to-cell transmission is more efficient both in vivo and in vitro (23, 42, 45, 61). Among drug abusers, HTLV-1 infection has been reported, indicating that HTLV-1 can be transmitted by the sharing of needles (12). Therefore, in cases of accidental exposure to HTLV-1-positive blood, preventive administration of antiretroviral drugs should be considered. In this study, we proved that the administration of a reverse transcriptase inhibitor beginning immediately after exposure can block HTLV-1 transmission. However, a delay in its administration may render it ineffective at preventing HTLV-1 transmission due to the importance of clonal expansion in the biology of this virus.

In particular, whether clonal expansion or internal continuous contagion is important in increasing the number of infected cells still remains unknown. A previous study reported that a reverse transcriptase inhibitor, lamivudine, reduced the proviral load in a patient with HAM/TSP (56), implicating internal contagion in maintaining the number of infected cells in vivo. However, another study reported that lamivudine had no definite effect on proviral load (34). In this study, administering tenofovir to block the spread of infection to new cells did not influence the proviral load in hu-PBMC-NOG mice, even though tenofovir has been reported to be more efficient in inhibiting HTLV-1 replication than lamivudine (20). Taken together, these results suggest that clonal proliferation contributes to the increase of HTLV-1-infected cells more than internal contagion even early in HTLV-1 infection. Recently, one study reported that clonality of HTLV-1-infected cells was variable after seroconversion but it became stable over time, indicating that the host immune system selected certain HTLV-1-infected clones (53). Since there is little or no host immune response to HTLV-1-infected cells in our system, it is possible that clonal proliferation of HTLV-1-infected cells is influenced by their ability to produce HTLV-1-encoded proteins, such as Tax. The factors including integration of the provirus in certain sites of the genome might also contribute to the variable proliferation of infected cells.

Viral gene transcription in HTLV-1-infected cells and ATL cells is suppressed in vivo. However, when they are cultured in vitro, transcription is rapidly recovered (54). Regarding the mechanisms of in vivo suppression, one possibility is that CTLs kill Tax-expressing cells, and the other is that nonimmune factors suppress it. The removal of $CD8^+$ T lymphocytes from PBMC derived from seropositive carriers enhanced Tax expression, suggesting that CTLs were indeed involved in inhibiting Tax expression in vivo (15, 18). On the other hand, a nonimmune factor(s) might be involved in this suppression. In this study, we showed that *tax* gene transcription was enhanced after in vitro culture. This finding is very similar to the phenomenon in carriers. It is noteworthy that in our system, there is no immune response to HTLV-1, indicating that a nonimmune factor(s) suppresses *tax* gene expression in vivo. These results suggest that both immune and nonimmune factors may be involved in the silencing of *tax* gene transcription.

Methylation of proviral DNA is regarded as a kind of host defense mechanism to suppress viral gene expression. However, HTLV-1 utilizes this epigenetic modification to escape the host immune surveillance. In cells immortalized by HTLV-1 in vitro, there was little DNA methylation in the provirus. In humans, on the other hand, DNA methylation accumulated within one year after seroconversion (54). In our system, DNA methylation was detected in the *pol* and *gag* regions 4 weeks after inoculation of MT-2 cells, indicating that HTLV-1 provirus is prone to methylation in vivo. Since *tax* gene transcription is silenced in hu-PBMC-NOG mice as shown in this study, such suppression might promote DNA methylation in vivo. On the other hand, since proliferation of HTLV-1-immortalized T lymphocytes is likely dependent on Tax expression, we speculate that cells with unmethylated provirus have growth advantages. We previously reported that histone H3 was hyperacetylated in the 5′ LTR of ATL cells without *tax* gene transcription, and such ATL cells transcribed *tax* gene within one hour after in vitro culture (54). This suggests the presence of a factor(s) inhibitory to *tax* gene transcription whose inhibition is nullified in in vitro culture. Such a mechanism, with the capacity for quickly switching on and off, would be useful for controlling *tax* gene transcription in vivo and thus enabling HTLV-1-infected cells to escape the host immune response.

In this study, we established an in vivo system for de novo infection with HTLV-1 and observed that the phenotype of HTLV-1-infected cells resembled that in the carrier state. The limitation of this in vivo system is that the long-term persistence of de novo infection in hu-PBMC-NOG mice cannot be examined, due to the graft-versus-host disease caused by implanted human lymphocytes. On the other hand, its merit is that the severe immune deficiency of this strain allows the vigorous proliferation of human lymphocytes, previously reported to be the result of a hyperactivation of the cells (40),

which enables HTLV-1 to rapidly spread by cell-to-cell contact. Therefore, this model system should be a useful tool for analyzing the events in the early stage of HTLV-1 infection in human lymphocytes.

ACKNOWLEDGMENTS

We thank Gilead Sciences Inc. for generously providing tenofovir for this study and Linda Kingsbury for excellent proofreading.

This study was supported by a grant-in-aid for scientific research from the Ministry of Education, Science, Sports, and Culture of Japan.

REFERENCES

1. **Akagi, T., I. Takeda, T. Oka, Y. Ohtsuki, S. Yano, and I. Miyoshi.** 1985. Experimental infection of rabbits with human T-cell leukemia virus type I. Jpn. J. Cancer Res. **76**:86–94.
2. **Albrecht, B., C. D. D'Souza, W. Ding, S. Tridandapani, K. M. Coggeshall, and M. D. Lairmore.** 2002. Activation of nuclear factor of activated T cells by human T-lymphotropic virus type 1 accessory protein $p12^{I}$. J. Virol. **76**:3493–3501.
3. **Arnold, J., B. Yamamoto, M. Li, A. J. Phipps, I. Younis, M. D. Lairmore, and P. L. Green.** 2006. Enhancement of infectivity and persistence in vivo by HBZ, a natural antisense coded protein of HTLV-1. Blood **107**:3976–3982.
4. **Bangham, C. R., and M. Osame.** 2005. Cellular immune response to HTLV-1. Oncogene **24**:6035–6046.
5. **Collins, N. D., G. C. Newbound, B. Albrecht, J. L. Beard, L. Ratner, and M. D. Lairmore.** 1998. Selective ablation of human T-cell lymphotropic virus type 1 p12I reduces viral infectivity in vivo. Blood **91**:4701–4707.
6. **Datta, S., N. H. Kothari, and H. Fan.** 2000. In vivo genomic footprinting of the human T-cell leukemia virus type 1 (HTLV-1) long terminal repeat enhancer sequences in HTLV-1-infected human T-cell lines with different levels of Tax I activity. J. Virol. **74**:8277–8285.
7. **Debacq, C., J. M. Heraud, B. Asquith, C. Bangham, F. Merien, V. Moules, F. Mortreux, E. Wattel, A. Burny, R. Kettmann, M. Kazanji, and L. Willems.** 2005. Reduced cell turnover in lymphocytic monkeys infected by human T-lymphotropic virus type 1. Oncogene **24**:7514–7523.
8. **Derse, D., S. A. Hill, P. A. Lloyd, H. Chung, and B. A. Morse.** 2001. Examining human T-lymphotropic virus type 1 infection and replication by cell-free infection with recombinant virus vectors. J. Virol. **75**:8461–8468.
9. **Dewan, M. Z., K. Terashima, M. Taruishi, H. Hasegawa, M. Ito, Y. Tanaka, N. Mori, T. Sata, Y. Koyanagi, M. Maeda, Y. Kubuki, A. Okayama, M. Fujii, and N. Yamamoto.** 2003. Rapid tumor formation of human T-cell leukemia virus type 1-infected cell lines in novel NOD-SCID/γc^{null} mice: suppression by an inhibitor against NF-κB. J. Virol. **77**:5286–5294.
10. **Etoh, K., S. Tamiya, K. Yamaguchi, A. Okayama, H. Tsubouchi, T. Ideta, N. Mueller, K. Takatsuki, and M. Matsuoka.** 1997. Persistent clonal proliferation of human T-lymphotropic virus type I-infected cells in vivo. Cancer Res. **57**:4862–4867.
11. **Fan, N., J. Gavalchin, B. Paul, K. H. Wells, M. J. Lane, and B. J. Poiesz.** 1992. Infection of peripheral blood mononuclear cells and cell lines by cell-free human T-cell lymphoma/leukemia virus type I. J. Clin. Microbiol. **30**:905–910.
12. **Feigal, E., E. Murphy, K. Vranizan, P. Bacchetti, R. Chaisson, J. E. Drummond, W. Blattner, M. McGrath, J. Greenspan, and A. Moss.** 1991. Human T cell lymphotropic virus types I and II in intravenous drug users in San Francisco: risk factors associated with seropositivity. J. Infect. Dis. **164**:36–42.
13. **Feuer, G., J. A. Zack, W. J. Harrington, Jr., R. Valderama, J. D. Rosenblatt, W. Wachsman, S. M. Baird, and I. S. Chen.** 1993. Establishment of human T-cell leukemia virus type I T-cell lymphomas in severe combined immunodeficient mice. Blood **82**:722–731.
14. **Franchini, G., R. Fukumoto, and J. R. Fullen.** 2003. T-cell control by human T-cell leukemia/lymphoma virus type 1. Int. J. Hematol. **78**:280–296.
15. **Furuta, R. A., K. Sugiura, S. Kawakita, T. Inada, S. Ikehara, T. Matsuda, and J. Fujisawa.** 2002. Mouse model for the equilibration interaction between the host immune system and human T-cell leukemia virus type 1 gene expression. J. Virol. **76**:2703–2713.
16. **Gessain, A., F. Barin, J. C. Vernant, O. Gout, L. Maurs, A. Calender, and G. de The.** 1985. Antibodies to human T-lymphotropic virus type-I in patients with tropical spastic paraparesis. Lancet **ii**:407–410.
17. **Grassmann, R., M. Aboud, and K. T. Jeang.** 2005. Molecular mechanisms of cellular transformation by HTLV-1 Tax. Oncogene **24**:5976–5985.
18. **Hanon, E., S. Hall, G. P. Taylor, M. Saito, R. Davis, Y. Tanaka, K. Usuku, M. Osame, J. N. Weber, and C. R. Bangham.** 2000. Abundant tax protein expression in CD4+ T cells infected with human T-cell lymphotropic virus type I (HTLV-I) is prevented by cytotoxic T lymphocytes. Blood **95**:1386–1392.
19. **Hanon, E., J. C. Stinchcombe, M. Saito, B. E. Asquith, G. P. Taylor, Y. Tanaka, J. N. Weber, G. M. Griffiths, and C. R. Bangham.** 2000. Fratricide among CD8(+) T lymphocytes naturally infected with human T cell lymphotropic virus type I. Immunity **13**:657–664.
20. **Hill, S. A., P. A. Lloyd, S. McDonald, J. Wykoff, and D. Derse.** 2003. Susceptibility of human T cell leukemia virus type I to nucleoside reverse transcriptase inhibitors. J. Infect. Dis. **188**:424–427.
21. **Hinuma, Y., Y. Gotoh, K. Sugamura, K. Nagata, T. Goto, M. Nakai, N. Kamada, T. Matsumoto, and K. Kinoshita.** 1982. A retrovirus associated with human adult T-cell leukemia: in vitro activation. Gann **73**:341–344.
22. **Hiraragi, H., S. J. Kim, A. J. Phipps, M. Silic-Benussi, V. Ciminale, L. Ratner, P. L. Green, and M. D. Lairmore.** 2006. Human T-lymphotropic virus type 1 mitochondrion-localizing protein $p13^{II}$ is required for viral infectivity in vivo. J. Virol. **80**:3469–3476.
23. **Igakura, T., J. C. Stinchcombe, P. K. Goon, G. P. Taylor, J. N. Weber, G. M. Griffiths, Y. Tanaka, M. Osame, and C. R. Bangham.** 2003. Spread of HTLV-I between lymphocytes by virus-induced polarization of the cytoskeleton. Science **299**:1713–1716.
24. **Imada, K., A. Takaori-Kondo, T. Akagi, K. Shimotohno, K. Sugamura, T. Hattori, H. Yamabe, M. Okuma, and T. Uchiyama.** 1995. Tumorigenicity of human T-cell leukemia virus type I-infected cell lines in severe combined immunodeficient mice and characterization of the cells proliferating in vivo. Blood **86**:2350–2357.
25. **Ito, M., H. Hiramatsu, K. Kobayashi, K. Suzue, M. Kawahata, K. Hioki, Y. Ueyama, Y. Koyanagi, K. Sugamura, K. Tsuji, T. Heike, and T. Nakahata.** 2002. NOD/SCID/gamma(c) (null) mouse: an excellent recipient mouse model for engraftment of human cells. Blood **100**:3175–3182.
26. **Johnson, J. M., C. Nicot, J. Fullen, V. Ciminale, L. Casareto, J. C. Mulloy, S. Jacobson, and G. Franchini.** 2001. Free major histocompatibility complex class I heavy chain is preferentially targeted for degradation by human T-cell leukemia/lymphotropic virus type 1 $p12^{I}$ protein. J. Virol. **75**:6086–6094.
27. **Kannagi, M., S. Harada, I. Maruyama, H. Inoko, H. Igarashi, G. Kuwashima, S. Sato, M. Morita, M. Kidokoro, M. Sugimoto, et al.** 1991. Predominant recognition of human T cell leukemia virus type I (HTLV-I) pX gene products by human CD8+ cytotoxic T cells directed against HTLV-I-infected cells. Int. Immunol. **3**:761–767.
28. **Kannagi, M., S. Matsushita, H. Shida, and S. Harada.** 1994. Cytotoxic T cell response and expression of the target antigen in HTLV-I infection. Leukemia **8**(Suppl. 1):S54–S59.
29. **Kim, S. J., A. M. Nair, S. Fernandez, L. Mathes, and M. D. Lairmore.** 2006. Enhancement of LFA-1-mediated T cell adhesion by human T lymphotropic virus type 1 p12I1. J. Immunol. **176**:5463–5470.
30. **Kinoshita, T., M. Shimoyama, K. Tobinai, M. Ito, S. Ito, S. Ikeda, K. Tajima, K. Shimotohno, and T. Sugimura.** 1989. Detection of mRNA for the tax1/rex1 gene of human T-cell leukemia virus type I in fresh peripheral blood mononuclear cells of adult T-cell leukemia patients and viral carriers by using the polymerase chain reaction. Proc. Natl. Acad. Sci. USA **86**:5620–5624.
31. **Koyanagi, Y., Y. Itoyama, N. Nakamura, K. Takamatsu, J. Kira, T. Iwamasa, I. Goto, and N. Yamamoto.** 1993. In vivo infection of human T-cell leukemia virus type I in non-T cells. Virology **196**:25–33.
32. **Lairmore, M. D., L. Silverman, and L. Ratner.** 2005. Animal models for human T-lymphotropic virus type 1 (HTLV-1) infection and transformation. Oncogene **24**:6005–6015.
33. **Li, H. C., R. J. Biggar, W. J. Miley, E. M. Maloney, B. Cranston, B. Hanchard, and M. Hisada.** 2004. Provirus load in breast milk and risk of mother-to-child transmission of human T lymphotropic virus type I. J. Infect. Dis. **190**:1275–1278.
34. **Machuca, A., B. Rodes, and V. Soriano.** 2001. The effect of antiretroviral therapy on HTLV infection. Virus Res. **78**:93–100.
35. **Manel, N., F. J. Kim, S. Kinet, N. Taylor, M. Sitbon, and J. L. Battini.** 2003. The ubiquitous glucose transporter GLUT-1 is a receptor for HTLV. Cell **115**:449–459.
36. **Matsuoka, M., and K. T. Jeang.** 2005. Human T-cell leukemia virus type I at age 25: a progress report. Cancer Res. **65**:4467–4470.
37. **Matsushita, S., H. Mitsuya, M. S. Reitz, and S. Broder.** 1987. Pharmacological inhibition of in vitro infectivity of human T lymphotropic virus type I. J. Clin. Investig. **80**:394–400.
38. **Michael, B., A. M. Nair, H. Hiraragi, L. Shen, G. Feuer, K. Boris-Lawrie, and M. D. Lairmore.** 2004. Human T lymphotropic virus type-1 p30II alters cellular gene expression to selectively enhance signaling pathways that activate T lymphocytes. Retrovirology **1**:39.
39. **Nagai, M., M. B. Brennan, J. A. Sakai, C. A. Mora, and S. Jacobson.** 2001. CD8(+) T cells are an in vivo reservoir for human T-cell lymphotropic virus type I. Blood **98**:1858–1861.
40. **Nakata, H., K. Maeda, T. Miyakawa, S. Shibayama, M. Matsuo, Y. Takaoka, M. Ito, Y. Koyanagi, and H. Mitsuya.** 2005. Potent anti-R5 human immunodeficiency virus type 1 effects of a CCR5 antagonist, AK602/ONO4128/GW873140, in a novel human peripheral blood mononuclear cell nonobese diabetic-SCID, interleukin-2 receptor gamma-chain-knocked-out AIDS mouse model. J. Virol. **79**:2087–2096.
41. **Nicot, C., M. Dundr, J. M. Johnson, J. R. Fullen, N. Alonzo, R. Fukumoto, G. L. Princler, D. Derse, T. Misteli, and G. Franchini.** 2004. HTLV-1-

encoded p30II is a post-transcriptional negative regulator of viral replication. Nat. Med. 10:197–201.
42. **Okochi, K., and H. Sato.** 1984. Transmission of ATLV (HTLV-I) through blood transfusion. Princess Takamatsu Symp. 15:129–135.
43. **Osame, M., K. Usuku, S. Izumo, N. Ijichi, H. Amitani, A. Igata, M. Matsumoto, and M. Tara.** 1986. HTLV-I associated myelopathy, a new clinical entity. Lancet i:1031–1032.
44. **Poiesz, B. J., F. W. Ruscetti, A. F. Gazdar, P. A. Bunn, J. D. Minna, and R. C. Gallo.** 1980. Detection and isolation of type C retrovirus particles from fresh and cultured lymphocytes of a patient with cutaneous T-cell lymphoma. Proc. Natl. Acad. Sci. USA 77:7415–7419.
45. **Popovic, M., P. S. Sarin, M. Robert-Gurroff, V. S. Kalyanaraman, D. Mann, J. Minowada, and R. C. Gallo.** 1983. Isolation and transmission of human retrovirus (human T-cell leukemia virus). Science 219:856–859.
46. **Richardson, J. H., A. J. Edwards, J. K. Cruickshank, P. Rudge, and A. G. Dalgleish.** 1990. In vivo cellular tropism of human T-cell leukemia virus type 1. J. Virol. 64:5682–5687.
47. **Silverman, L. R., A. J. Phipps, A. Montgomery, L. Ratner, and M. D. Lairmore.** 2004. Human T-cell lymphotropic virus type 1 open reading frame II-encoded $p30^{II}$ is required for in vivo replication: evidence of in vivo reversion. J. Virol. 78:3837–3845.
48. **Sugiyama, H., H. Doi, K. Yamaguchi, Y. Tsuji, T. Miyamoto, and S. Hino.** 1986. Significance of postnatal mother-to-child transmission of human T-lymphotropic virus type-I on the development of adult T-cell leukemia/lymphoma. J. Med. Virol. 20:253–260.
49. **Tajima, K., S. Tominaga, and T. Suchi.** 1986. Malignant lymphomas in Japan: epidemiological analysis on adult T-cell leukemia/lymphoma. Hematol. Oncol. 4:31–44.
50. **Takatsuki, K.** 2005. Discovery of adult T-cell leukemia. Retrovirology 2:16.
51. **Takatsuki, K., T. Uchiyama, K. Sagawa, and J. Yodoi.** 1977. Adult T cell leukemia in Japan, p. 73–77. *In* S. Seno, F. Takaku, and S. Irino (ed.), Topic in hematology. The 16th International Congress of Hematology. Excerpta Medica, Amsterdam, The Netherlands.
52. **Takeda, S., M. Maeda, S. Morikawa, Y. Taniguchi, J. Yasunaga, K. Nosaka, Y. Tanaka, and M. Matsuoka.** 2004. Genetic and epigenetic inactivation of tax gene in adult T-cell leukemia cells. Int. J. Cancer 109:559–567.
53. **Tanaka, G., A. Okayama, T. Watanabe, S. Aizawa, S. Stuver, N. Mueller, C. C. Hsieh, and H. Tsubouchi.** 2005. The clonal expansion of human T lymphotropic virus type 1-infected T cells: a comparison between seroconverters and long-term carriers. J. Infect. Dis. 191:1140–1147.
54. **Taniguchi, Y., K. Nosaka, J. Yasunaga, M. Maeda, N. Mueller, A. Okayama, and M. Matsuoka.** 2005. Silencing of human T-cell leukemia virus type I gene transcription by epigenetic mechanisms. Retrovirology 2:64.
55. **Tateno, M., N. Kondo, T. Itoh, T. Chubachi, T. Togashi, and T. Yoshiki.** 1984. Rat lymphoid cell lines with human T cell leukemia virus production. I. Biological and serological characterization. J. Exp. Med. 159:1105–1116.
56. **Taylor, G. P., S. E. Hall, S. Navarrete, C. A. Michie, R. Davis, A. D. Witkover, M. Rossor, M. A. Nowak, P. Rudge, E. Matutes, C. R. Bangham, and J. N. Weber.** 1999. Effect of lamivudine on human T-cell leukemia virus type 1 (HTLV-1) DNA copy number, T-cell phenotype, and anti-Tax cytotoxic T-cell frequency in patients with HTLV-1-associated myelopathy. J. Virol. 73:10289–10295.
57. **Uchiyama, T.** 1997. Human T cell leukemia virus type I (HTLV-I) and human diseases. Annu. Rev. Immunol. 15:15–37.
58. **Uchiyama, T., J. Yodoi, K. Sagawa, K. Takatsuki, and H. Uchino.** 1977. Adult T-cell leukemia: clinical and hematologic features of 16 cases. Blood 50:481–492.
59. **Xiong, Z., and P. W. Laird.** 1997. COBRA: a sensitive and quantitative DNA methylation assay. Nucleic Acids Res. 25:2532–2534.
60. **Yahata, T., K. Ando, Y. Nakamura, Y. Ueyama, K. Shimamura, N. Tamaoki, S. Kato, and T. Hotta.** 2002. Functional human T lymphocyte development from cord blood CD34+ cells in nonobese diabetic/Shi-scid, IL-2 receptor gamma null mice. J. Immunol. 169:204–209.
61. **Yamamoto, N., M. Okada, Y. Koyanagi, M. Kannagi, and Y. Hinuma.** 1982. Transformation of human leukocytes by cocultivation with an adult T cell leukemia virus producer cell line. Science 217:737–739.
62. **Yasunaga, J., T. Sakai, K. Nosaka, K. Etoh, S. Tamiya, S. Koga, S. Mita, M. Uchino, H. Mitsuya, and M. Matsuoka.** 2001. Impaired production of naive T lymphocytes in human T-cell leukemia virus type I-infected individuals: its implications in the immunodeficient state. Blood 97:3177–3183.
63. **Yoshida, M.** 2001. Multiple viral strategies of HTLV-1 for dysregulation of cell growth control. Annu. Rev. Immunol. 19:475–496.
64. **Zhang, W., J. W. Nisbet, B. Albrecht, W. Ding, F. Kashanchi, J. T. Bartoe, and M. D. Lairmore.** 2001. Human T-lymphotropic virus type 1 $p30^{II}$ regulates gene transcription by binding CREB binding protein/p300. J. Virol. 75:9885–9895.
65. **Zhao, T. M., B. Hague, D. L. Caudell, R. M. Simpson, and T. J. Kindt.** 2005. Quantification of HTLV-I proviral load in experimentally infected rabbits. Retrovirology 2:34.

Donor-Derived T-Cell Leukemia after Bone Marrow Transplantation

TO THE EDITOR: Asymptomatic carriers of human T-cell lymphotropic virus type I (HTLV-I) are considered acceptable as donors in allogeneic stem-cell transplantation for patients with adult T-cell leukemia–lymphoma (ATL).[1] However, the infusion of HTLV-I–infected cells from HTLV-I–seropositive donors could lead to the development of donor-derived ATL under immunosuppressive conditions after stem-cell transplantation. Here we describe a patient in whom ATL derived from donor cells developed four months after transplantation of stem cells from a sibling with HTLV-I.

A 44-year-old Japanese man with lymphoma-type ATL underwent transplantation of bone marrow from his HLA-identical brother in February 2004. The conditioning regimen included intravenous cyclophosphamide (120 mg per kilogram of body weight) and total-body irradiation (12 Gy). Cyclosporine and a short course of methotrexate were given as prophylaxis against graft-versus-host disease (GVHD). On day 26, low-dose prednisone was instituted because of GVHD-associated fever. With stable hematopoietic engraftment, complete donor chimerism was confirmed in a T-cell fraction on day 20 (Fig. 1). On day 133, the patient's white-cell count increased to 49.1×10^9 per liter with 89 percent ATL cells, although the original tumor had completely disappeared. Southern blot analysis revealed monoclonal integration of HTLV-I provirus in the ATL cells. Although we discontinued immunosuppressive therapy and administered chemotherapeutic agents, the patient died of the tumor in August 2004 (day 177).

A test for the status of donor–recipient chimerism in a T-cell–enriched fraction at the onset of ATL after transplantation showed a donor pattern (Fig. 1). In September 2004, hematologic and blood chemical values of the donor were almost normal, although the white-cell count included 1 percent atypical lymphocytes. Southern blot analysis showed no monoclonal integration of the HTLV-I provirus in the peripheral-blood mononuclear cells of the donor. These findings suggest that the donor was still an asymptomatic carrier without substantial clonal proliferation of HTLV-I–infected cells.

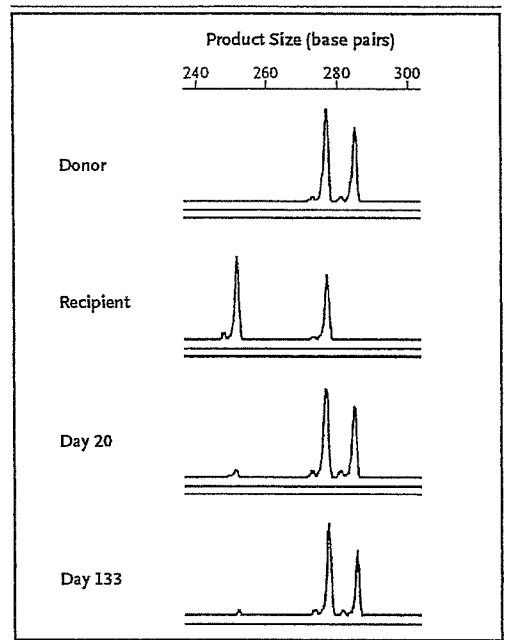

Figure 1. Analysis of T Cells at Engraftment (Day 20) and at the Onset of ATL (Day 133).

Genomic DNA from peripheral blood was amplified by polymerase-chain-reaction (PCR) assays with the use of fluorescent primers flanking an informative microsatellite region. Fluorescent peak controls for the donor and the recipient before stem-cell transplantation were obtained from whole peripheral-blood cells. At the onset of ATL after stem-cell transplantation, enriched CD3-positive cells, which were obtained with a purity of more than 95 percent, showed typical morphologic features of ATL cells on blood smears, and most of them expressed both CD4 and CD25, as assessed by flow cytometry. Fluorescent PCR products and GeneScan ROX 500 Size Standard were analyzed in a genetic analyzer with the use of Genescan software (Version 3.1.2) (ABI-310, Applied Biosystems).

Suppression of the host immune system increases the occurrence of virus-associated lymphoid cancers.[2] ATL develops in approximately 5 percent of HTLV-I carriers after an incubation period of several decades.[3] However, ATL has been reported to develop at a younger age in renal-transplant recipients with HTLV-I infection during immunosuppressive therapy[4] and sooner after the transmission of HTLV-I infection through blood transfusion in patients under immunosuppressive conditions.[5] Thus, the immunosuppressive

status in recipients of stem-cell transplants also potentially contributes to the development of ATL in donor-derived T cells that are infected with HTLV-I.

Hiroya Tamaki, M.D., Ph.D.
Osaka Minami Medical Center
Osaka 586-8521, Japan
tamaki@ommc-hp.jp

Masao Matsuoka, M.D., Ph.D.
Kyoto University Institute for Virus Research
Kyoto 606-8507, Japan

1. Utsunomiya A, Miyazaki Y, Takatsuka Y, et al. Improved outcome of adult T cell leukemia/lymphoma with allogeneic hematopoietic stem cell transplantation. Bone Marrow Transplant 2001; 27:15-20.
2. Cohen JI. Epstein–Barr virus infection. N Engl J Med 2000; 343:481-92.
3. Matsuoka M. Human T-cell leukemia virus type I and adult T-cell leukemia. Oncogene 2003;22:5131-40.
4. Hoshida Y, Li T, Dong Z, et al. Lymphoproliferative disorders in renal transplant patients in Japan. Int J Cancer 2001;91:869-75.
5. Chen YC, Wang CH, Su IJ, et al. Infection of human T-cell leukemia virus type I and development of human T-cell leukemia lymphoma in patients with hematologic neoplasms: a possible linkage to blood transfusion. Blood 1989;74:388-94.

A Case of Platydeoxia?

TO THE EDITOR: The Clinical Problem-Solving article by Hegland et al. (Dec. 1 issue)[1] concerned a case of platypnea–orthodeoxia, in which a positionally dependent intracardiac right-to-left shunt led to arterial desaturation when the patient was in the upright position but not the supine. We report a case in which the converse occurred.

An 81-year-old woman was brought to the emergency room by her neighbors, who found her lying on the floor of her apartment, markedly confused. On examination, the patient was cooperative but delirious. She was hemodynamically stable, her respiratory rate was 13 breaths per minute, and her initial oxygen saturation was 95 percent while breathing room air. Repeated oximetry several hours later revealed an oxygen saturation of 80 percent and blood gas measurement yielded a partial pressure of arterial oxygen (PaO_2) of 34 mm Hg that did not improve despite the delivery of high-flow oxygen by aerosol mask. The patient was intubated and transferred to the intensive care unit. A spiral computed tomographic scan was negative for pulmonary embolism but revealed a very large aneurysm in the ascending aorta (8.2 cm by 8.0 cm) that was compressing the right main pulmonary artery.

In the intensive care unit, the patient was placed in a sitting position and the PaO_2 increased to 486 mm Hg. Her PaO_2 remained elevated despite the reduction of the fraction of inspired oxygen (F_IO_2) to 35 percent, and she was extubated and transferred back to the ward. On the ward, her oxygen saturation dropped to 60 percent and rose only marginally while she was breathing supplemental oxygen. It was then noted that the oxygen saturation rapidly corrected to 100 percent when the patient was placed lying on her side or sitting upright. A transthoracic echocardiogram with bubble study was performed; it revealed a patent

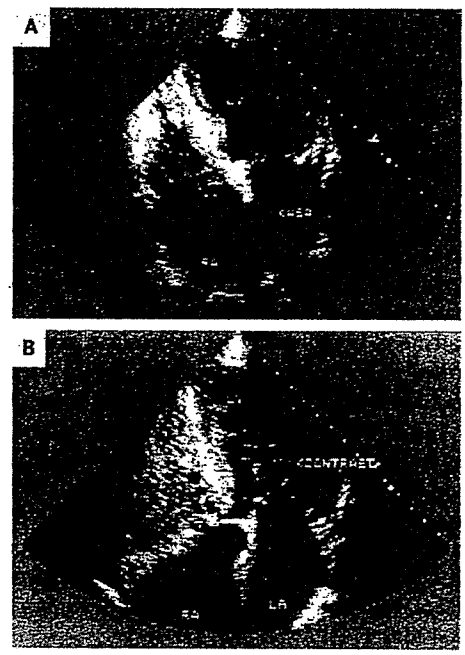

Figure 1. Transthoracic Echocardiography with Microbubble Contrast.

Panel A shows the echocardiogram that was obtained with the patient in the left lateral decubitus position and shows abundant microbubbles in the right atrium (RA) and only a few in the left ventricle (LV). ASA denotes atrial septal aneurysm. The echocardiogram in Panel B was obtained while the patient was in the supine position and shows the increased presence of microbubbles in the left atrium (LA) and left ventricle (LV).

Oncogene (2006) 25, 2181–2191

www.nature.com/onc

ORIGINAL ARTICLE

Loss of interleukin-2-dependency in HTLV-I-infected T cells on gene silencing of thioredoxin-binding protein-2

MK Ahsan[1], H Masutani[1], Y Yamaguchi[1], Y-C Kim[1], K Nosaka[2], M Matsuoka[2], Y Nishinaka[1], M Maeda[1] and J Yodoi[1]

[1]Department of Biological Responses, Institute for Virus Research, Kyoto University, Shogoin, Kawahara-cho, Sakyo-ku, Kyoto, Japan; [2]Research Center for Acquired Immunodeficiency Syndrome, Institute for Virus Research, Kyoto University, Shogoin, Kawahara-cho, Sakyo-ku, Kyoto, Japan

The transition from interleukin-2 (IL-2)-dependent to IL-2-independent growth is considered one of the key steps in the transformation of human T-cell leukemia virus type-I (HTLV-I)-infected T cells. The expression of thioredoxin-binding protein-2 (TBP-2) is lost during the transition of HTLV-I-infected T-cell lines. Here, we analysed the mechanism of loss of TBP-2 expression and the role of TBP-2 in IL-2-dependent growth in the *in vitro* model to investigate multistep transformation of HTLV-I. CpGs in the *TBP-2* gene are methylated in IL-2-independent but not in IL-2-dependent cells. Sequential treatment with 5-aza-2′-deoxycytidine and a histone deacetylase inhibitor augmented histone acetylation and TBP-2 expression, suggesting that loss of TBP-2 expression is due to DNA methylation and histone deacetylation. In IL-2-dependent cells, a basal level of TBP-2 expression was maintained by IL-2 associated with cellular growth, whereas TBP-2 expression was upregulated on deprivation of IL-2 associated with growth suppression. Overexpression of TBP-2 in IL-2-independent cells suppressed the growth and partially restored responsiveness to IL-2. Knockdown of TBP-2 caused the IL-2-dependent cells to show partial growth without IL-2. These results suggested that epigenetic silencing of the *TBP-2* gene results in a loss of responsiveness to IL-2, contributing to uncontrolled IL-2-independent growth in HTLV-I-infected T-cell lines.

Oncogene (2006) **25**, 2181–2191. doi:10.1038/sj.onc.1209256; published online 28 November 2005

Keywords: HTLV-I; ATL; TBP-2/VDUP1; DNA-methylation; histone deacetylation; interleukin-2

Correspondence: Dr H Masutani, Department of Biological Responses, Institute for Virus Research, Kyoto University, 53 Shogoin, Kawahara-cho, Sakyo-ku, Kyoto 606-8507, Japan.
E-mail: hmasutan@virus.kyoto-u.ac.jp
Received 16 May 2005; revised 19 September 2005; accepted 17 October 2005; published online 28 November 2005

Introduction

Adult T-cell leukemia (ATL) is a disease entity with characteristic clinical and immunological features (Yodoi *et al.*, 1974; Uchiyama *et al.*, 1977), caused by human T-cell leukemia virus type-I (HTLV-I; Yoshida *et al.*, 1982). The long latent period and the age-dependent accumulation of leukemogenic events within HTLV-I-infected T cells suggest that the development of ATL is a multistep process (Okamoto *et al.*, 1989; Matsuoka, 2003). HTLV-I-infected T cells generally grow only in the presence of interleukin-2 (IL-2) (IL-2-dependent phase/IL-2-dependent cells; Maeda, 1992). But when these cells are cultured with IL-2 for several months, some fractions become able to proliferate continuously in the absence of IL-2 (IL-2-independent phase/IL-2-independent cells; Morgan *et al.*, 1976). The transition from the IL-2-dependent phase to IL-2-independent phase is an *in vitro* model for investigating the multistep process of the malignant transformation of HTLV-I-infected T cells (Maeda *et al.*, 1985; Migone *et al.*, 1995). ATL-derived factor (ADF) was cloned from HTLV-I-infected T cells (Tagaya *et al.*, 1989) and revealed to be a human homologue of thioredoxin (TRX; Holmgren, 1985). TRX is an oxidoreductase with important regulatory roles in cell proliferation and signal transduction (Masutani and Yodoi, 2002). TRX expression is markedly enhanced in HTLV-I-infected T cells (Makino *et al.*, 1992). Using the yeast two-hybrid screening system, we identified thioredoxin-binding protein-2 (TBP-2; Nishiyama *et al.*, 1999), which is identical to vitamin D_3 upregulated protein 1 (VDUP1; Chen and DeLuca, 1994). We have reported that TBP-2 has growth suppressive activity (Nishinaka *et al.*, 2004a) and its expression is abrogated in HTLV-I-infected IL-2-independent T cells, but maintained in HTLV-I-infected IL-2-dependent T cells as well as in HTLV-I-negative T cells (Nishinaka *et al.*, 2004a). TBP-2 expression is also downregulated in human cancers (Butler *et al.*, 2002; Han *et al.*, 2003). However, the mechanisms for the downregulation of TBP-2 expression remain unaddressed. In this study, we have investigated the mechanism of loss of TBP-2 expression in IL-2-independent HTLV-I-infected T-cell lines. We have also analysed the role of TBP-2 in IL-2-dependent growth control in HTLV-I-infected T-cell lines.

Results

Treatment with a demethylating reagent 5-aza-2′-deoxycytidine (5-aza-CdR) restored TBP-2 mRNA expression in HTLV-I-infected IL-2-independent cells

In the early stages of culture, HTLV-I-infected T cells generally grow only in the presence of IL-2 (IL-2-dependent cells). When these cells are cultured in the presence of IL-2 for several months; however, some fractions become able to proliferate continuously in the absence of IL-2 (IL-2-independent cells) (Morgan *et al.*, 1976; Maeda, 1992). Each set of IL-2-dependent and IL-2-independent cells has the same clonal origin as confirmed by the T-cell receptor-β gene rearrangement and HTLV-I proviral integration sites (Maeda, 1992). We analysed the expression of TBP-2 mRNA in sets of IL-2-dependent and IL-2-independent cells. The expression was lost in IL-2-independent cells (ATL-2, ED-40515, ATL-35T and ATL-43T) but not in IL-2-dependent cells (Figure 1a). However, we did not find genetic alterations in the promoter or coding region of the *TBP-2* gene (data not shown). The *TBP-2* promoter region nearest the TATA-box contained more than 49% GC and the observed CpG (number of CpG multiplied by total number of nucleotides of the region)/expected CpG (number of C multiplied by total number of nucleotides of the region) ratio was 0.64. The CpG/GpC ratio was 1. These values are considered sufficient to meet the criteria for CpG-dinucleotides susceptible to methylation (Gardiner-Garden and Frommer, 1987). Since hyper-methylation of promoter CpG-dinucleotides is often associated with inactivation of gene transcription, we first examined whether the *TBP-2* gene is methylated by testing the effect of a demethylating reagent, 5-aza-CdR, on TBP-2 expression in IL-2-independent ATL-43T and ATL-2 cells. Consistent with a previous report (Nosaka *et al.*, 2000), treatment with 5-aza-CdR restored CDKN2A gene expression (Figure 1b, mid gel). The treatment also restored the mRNA expression of TBP-2 in the cells (Figure 1b, upper gel, and 1c). To further examine the methylation status of the *TBP-2* promoter region, we directly sequenced the genomic DNA after treatment with sodium bisulfite. Sodium bisulfite converts C to T, except the C of methylated CpG. As shown in Figure 2, the CpGs in the promoter region and exon-1 of *TBP-2* were heavily methylated in IL-2-independent ATL cell lines, compared with those in IL-2-dependent cell lines. On treatment with 5-aza-CdR, about one-third of the methylated CpGs were demethylated in IL-2-independent ATL-43T and ATL-2 cells. These results strongly suggested that DNA methylation is involved in the mechanism of abrogation of TBP-2 mRNA expression in HTLV-I-infected IL-2-independent cells.

Involvement of histone deacetylation in TBP-2 gene silencing in HTLV-I-infected IL-2-independent cells

The restoration of TBP-2 expression by 5-aza-CdR in IL-2-independent cells seemed to be partial. Moreover, DNA methylation and histone deacetylation are

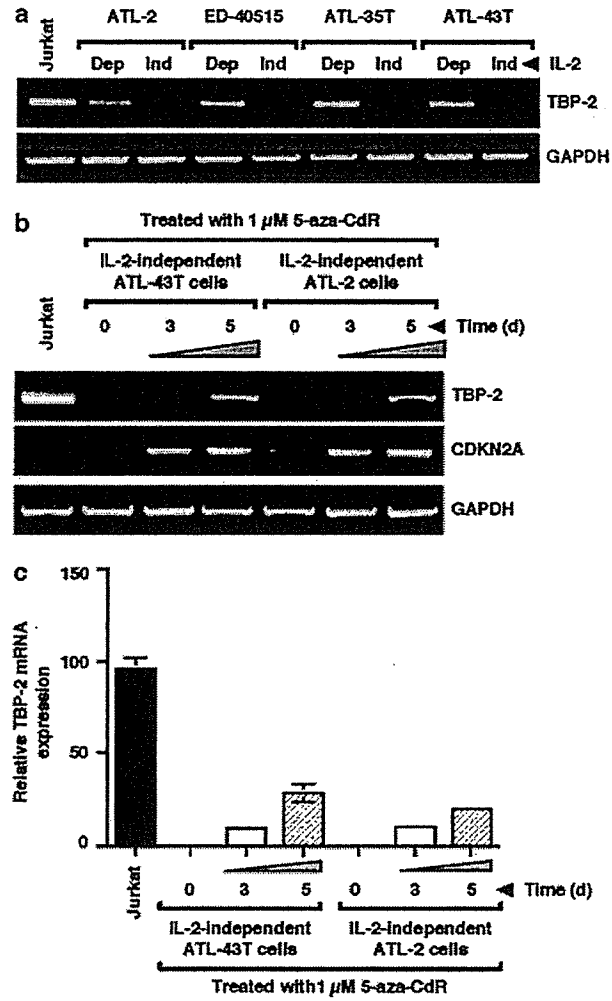

Figure 1 Restoration of thioredoxin-binding protein-2 (*TBP-2*) expression by 5-aza-2′-deoxycytidine (*5-aza-CdR*) in interleukin-2 (IL-2)-independent HTLV-I-infected T cells. An equivalent amount of total RNA was analysed by semiquantitative RT–PCR. GAPDH was amplified as an internal control. (a) Loss of TBP-2 expression in the HTLV-I-infected IL-2-independent T cells. *Dep*: IL-2-dependent cells and *Ind*: IL-2-independent cells. (b) Restoration of TBP-2 expression by 5-aza-CdR. IL-2-independent ATL-43T and ATL-2 cells were treated with 1 μM 5-aza-CdR for 0, 3 or 5 days and expression levels of TBP-2 and CDKN2A were analysed by semiquantitative RT–PCR. (c) Quantitative real-time RT–PCR analysis of TBP-2 mRNA expression. Data are representative of three separate experiments and the mean$\pm$s.d. from three replicates. 18S ribosomal mRNA expression was used as a cDNA loading control.

dynamically linked and synergistically silenced tumor suppressor genes (Cameron *et al.*, 1999). Therefore, we next analysed whether histone deacetylation is involved in *TBP-2* gene silencing. Treatment with suberoylanilide hydroxamic acid (SAHA), a histone deacetylase (HDAC) inhibitor, alone was unable to restore TBP-2 expression in IL-2-independent ATL-43T and ATL-2 cells (Figure 3a). Then, the cells were sequentially treated with 5-aza-CdR and SAHA. TBP-2 gene expression was restored by treatment with 5-aza-CdR

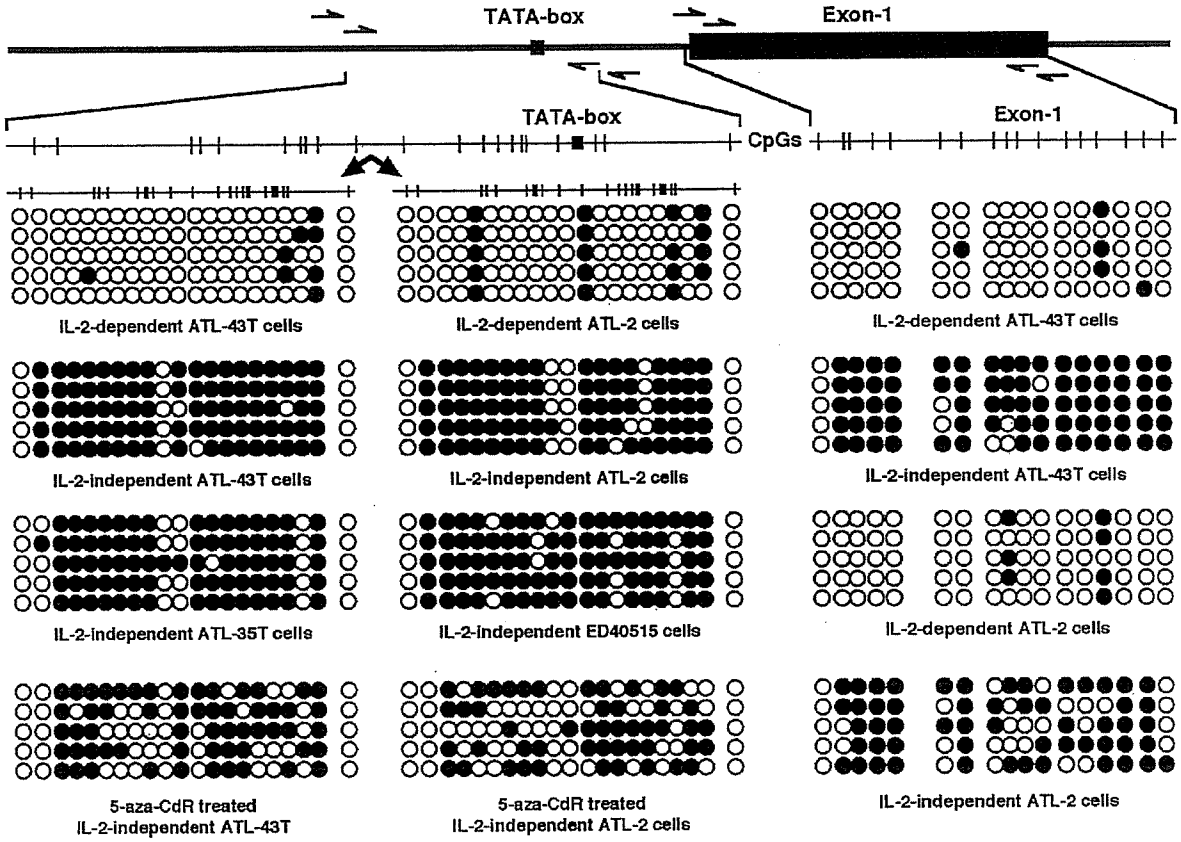

Figure 2 Methylation status of the thioredoxin-binding protein-2 (*TBP-2*) gene in HTLV-I-infected T-cell lines. Genomic DNA from HTLV-I-transformed IL-2-dependent and IL-2-independent cells before and after treatment with 5-aza-CdR were subjected to sodium bisulfite sequencing analyses as described in 'Materials and methods'. O, unmethylated CpG sites; •, methylated CpG sites.

for 3 days (Figure 3b, upper gel: lanes 3–5 and lanes 8–10), and further enhanced by additional treatment with SAHA for 1 day (Figure 3b, upper gel: lanes 6 and 11) in IL-2-independent ATL-43T and ATL-2 cells. The expression of TRX was not significantly altered by this treatment (Figure 3b, mid gel). These results suggested that both DNA-methylation and histone deacetylation synergistically silence the *TBP-2* gene in HTLV-I-infected IL-2-independent cells. In an earlier report (Butler *et al.*, 2002), SAHA augmented TBP-2 expression through the CCAAT element of the *TBP-2* promoter. However, SAHA alone was unable to restore the TBP-2 expression in our cases. To clarify whether the effect of SAHA is a cancellation of histone deacetylation, we performed a chromatin immunoprecipitation (Chip) assay in IL-2-independent ATL-43T and ATL-2 cells. The PCR signal obtained using anti-acetylated-H3 or H4 antibody was very weak in IL-2-independent ATL-43T and ATL-2 cells, before treatment or on treatment with SAHA only (Figure 3c). After treatment with 5-aza-CdR, the PCR signal was markedly enhanced. Sequential treatment with 5-aza-CdR and SAHA further strengthened the PCR signal. These results strongly suggested that DNA methylation and histone deacetylation are synergistically involved in the *TBP-2* gene silencing in HTLV-I-infected IL-2-independent cell lines.

Association between downregulation of TBP-2 expression in response to IL-2 and cellular growth

Augmented TBP-2 expression results in growth suppression (Nishinaka *et al.*, 2004a, b). We then analysed the relation between TBP-2 expression and growth in response to IL-2. We examined the level of TBP-2 expression and cell growth using [^{3}H]thymidine (Figure 4; ATL-43 T cells) and the MTT assay (Figure 5; ATL-2 cells). In IL-2-dependent ATL-43T (Figure 4a) and ATL-2 (Figure 5a) cells, TBP-2 expression was minimally maintained by the addition of IL-2, associated with cellular proliferation, whereas it was upregulated on deprivation of IL-2, associated with cell growth suppression. TBP-2 expression was recovered by sequential treatment with 5-aza-CdR and SAHA in IL-2-independent ATL-43T (Figure 4c) and ATL-2 (Figure 5c) cells. The expression of TBP-2 was also quantitated using real time RT–PCR (Figures 4d and 5d). These cells displayed a similar pattern of TBP-2 expression and growth in response to IL-2, mimicking that of IL-2-dependent cells. In contrast, IL-2-independent ATL-43T (Figure 4b) and ATL-2 (Figure 5b) cells